

UC Berkeley

UC Berkeley Previously Published Works

Title

Role of seasonal transitions and westerly jets in East Asian paleoclimate

Permalink

<https://escholarship.org/uc/item/1qz5g5j1>

Authors

Chiang, John CH

Fung, Inez Y

Wu, Chi-Hua

et al.

Publication Date

2015

DOI

10.1016/j.quascirev.2014.11.009

Peer reviewed

1
2
3
4
5
6
7
8
9
10
11
12
13
14
15
16
17
18
19
20
21
22
23

Role of Seasonal Transitions and Westerly Jets in East Asian Paleoclimate

John C. H. Chiang^{1,2,3}, Inez Y. Fung⁴, Chi-Hua Wu², Yanjun Cai⁵, Jacob P. Edman^{4,6}, Yuwei Liu¹, Jesse A. Day⁴, Tripti Bhattacharya¹, Yugarshi Mondal¹, and Clothilde A. Labrousse¹

¹ Dept. of Geography, University of California, Berkeley, CA, USA

² Research Center for Environmental Changes, Academia Sinica, Taipei, Taiwan

⁴ Dept. of Earth and Planetary Sciences, University of California, Berkeley CA, USA

⁵ The State Key Laboratory of Loess and Quaternary Geology, Institute of Earth Environment, Chinese Academy of Sciences, Xi'an, China

⁶ Earth Sciences Division, Lawrence Berkeley National Laboratory, Berkeley, CA, USA

Version date: November 15, 2014

Revised for Quaternary Science Reviews

³ Corresponding author address:
547 McCone Hall
University of California
Berkeley CA 94720-4740 USA
Email: jch_chiang@berkeley.edu

24 **Abstract**

25 The summer rainfall climate of East Asia underwent large and abrupt changes during past
26 climates, in response to precessional forcing, glacial-interglacial cycles as well as abrupt changes
27 to the North Atlantic during the last glacial. However, current interpretations of said changes are
28 typically formulated in terms of modulation of summer monsoon intensity, and do not account
29 for the known complexity in the seasonal evolution of East Asian rainfall, which exhibits sharp
30 transition from the Spring regime to the Meiyu, and then again from the Meiyu to the Summer
31 regime.

32 We explore the interpretation that East Asian rainfall climate undergoes a modulation of its
33 seasonality during said paleoclimate changes. Following previous suggestions we focus on role
34 of the westerly jet over Asia, namely that its latitude relative to Tibet is critical in determining
35 the stepwise transitions in East Asian rainfall seasons. In support of this linkage, we show from
36 observational data that the interannual co-variation of June (July-August) rainfall and upper
37 tropospheric zonal winds show properties consistent with an altered timing of the transition to
38 the Meiyu (Summer), and with more northward-shifted westerlies for earlier transitions.

39 We similarly suggest that East Asian paleoclimate changes resulted from an altered timing in
40 the northward evolution of the jet and hence the seasonal transitions, in particular the transition
41 of the jet from south of the Plateau to the north that determines the seasonal transition from
42 Spring rains to the Meiyu. In an extreme scenario – which we speculate the climate system
43 tended towards during stadial (cold) phases of D/O stadials and periods of low Northern
44 Hemisphere summer insolation – the jet does not jump north of the Plateau, essentially keeping
45 East Asia in prolonged Spring conditions.

46 We argue that this hypothesis provides a viable explanation for a key paleoproxy signature of

47 D/O stadials over East Asia, namely the heavier mean $\delta^{18}\text{O}$ of precipitation as recorded in
48 speleothem records. The southward jet position prevents the low-level monsoonal flow – which
49 is isotopically light – from penetrating into the interior of East Asia; as such, precipitation there
50 will be heavier, consistent with speleothem records. This hypothesis can also explain other key
51 evidences of East Asian paleoclimate changes, in particular the occurrence of dusty conditions
52 during North Atlantic stadials, and the southward migration of the Holocene optimal rainfall.

53 **1. Introduction**

54 East Asia experienced large and abrupt climate changes during the Pleistocene. The most
55 remarkable recent evidence of these changes is from stable oxygen isotope ratios ($\delta^{18}\text{O}$) of
56 speleothem calcium carbonate across various East Asian caves [*Wang et al.*, 2001; *Wang et al.*,
57 2008] (**figure 1**). They show large fluctuations in the $\delta^{18}\text{O}$ on millennial and precessional
58 timescales, with heavier isotopic composition during stadials, and similar fluctuations during
59 periods of low Northern Hemisphere (NH) summer insolation due to precessional changes in the
60 Earth's orbit. Other records corroborate the sense of large and abrupt change in East Asia; for
61 example, paleoproxy dust records show East Asia to be dustier during cold stadials (and in
62 particular Heinrich stadials) [*An et al.*, 2012; *Nagashima et al.*, 2011], and more generally during
63 glacial periods [*An*, 2000].

64 The dominant interpretation of variability in the speleothem records is as a record of
65 changes in East Asian summer monsoon intensity, with $\delta^{18}\text{O}$ relatively light when monsoons are
66 more intense [*Clemens et al.*, 2010; *Wang et al.*, 2001; *Wang et al.*, 2008]. This interpretation
67 originated with the 'amount effect' [*Dansgaard*, 1964] wherein rainfall is observed to be
68 isotopically lighter with stronger rainfall. However, while this relationship works well for
69 convective rainfall where evaporation exceeds precipitation [*Lee and Fung*, 2008], recent studies
70 from instrumental measurements over East Asia examining the variation of $\delta^{18}\text{O}$ find the amount
71 effect influence to be relatively weak on the whole and heterogeneous in space [*Dayem et al.*,
72 2010; *Johnson and Ingram*, 2004; *Lee et al.*, 2012]; moreover there is significant temperature
73 dependence of $\delta^{18}\text{O}$, especially at the northern extremities of the East Asian summer monsoon
74 region. Recent interpretations instead invoke seasonality where lighter $\delta^{18}\text{O}$ indicates relatively
75 more summer rainfall following from the fact that summer monsoon rainfall has lighter $\delta^{18}\text{O}$

76 than the rest of the year [Wang et al. 2001]. Following this logic, Cheng et al. [2009b] interpret
77 the speleothem record as a measure of the amount of summer monsoon precipitation, or as they
78 refer to as ‘summer monsoon intensity’.

79 Even if this were correct, the ‘summer monsoon intensity’ interpretation is at best
80 incomplete as it neglects the complexity of the seasonal evolution in East Asian rainfall. The
81 behavior of ‘typical’ monsoons - such as the West African or South Asian monsoon - are
82 characterized by the onset and retreat of one (summer) rainy season. East Asia spring and
83 summer rainfall, on the other hand, is characterized by several quasi-stationary stages and abrupt
84 transitions in between (see section 2).

85 We seek a more concrete interpretation of the East Asian paleo rainfall changes that
86 incorporates the complexity of the seasonal cycle. The role of seasonality and seasonal
87 transitions has been previously invoked in several previous East Asian paleoclimate studies,
88 though none of them comprehensively. An et al. [2000] argued for stepwise changes to the East
89 Asian monsoon during the Holocene whereby the region experiencing its ‘Holocene optimal’
90 (maximum rainfall during the course of the Holocene) shift with the phase of precession: peak
91 rainfall was attained during 10,000–7000 yr ago in north-central and northern east-central China;
92 ca. 7000–5000 yr ago in the middle and lower reaches of the Yangtze River; and ca. 3000 yr ago
93 in southern China. Clemens et al. [2010] argued for significant contributions of wintertime East
94 Asian rainfall in order to explain the phasing of East Asian precipitation relative to its South
95 Asian counterparts. Following the summer/non-summer rainfall ratio interpretation by Wang et
96 al. [2001] and Cheng et al. [2009b], Dayem et al. [2010] also explored the ramifications of
97 changes in the seasonality of precipitation on precipitation $\delta^{18}\text{O}$.

98 The quasi-stationary stages of East Asian rainfall and abrupt transitions indicates a
99 *dynamic* seasonality driven by circulation changes, and not simply a continuous response to
100 increasing insolation; moreover, it suggests that the dynamics underlying such changes could be
101 usefully applied to the paleoclimate scenarios. The view we promote is centered on the role of
102 the westerly jet impinging on Tibet; modern-day dynamical studies point to the seasonal north-
103 south evolution of the jet as playing a key role in the abrupt transitions in the East Asian rainfall
104 climate. It also turns out (as we will argue) that the meridional position of jet is sensitive to
105 many paleoclimate influences, including orbital changes, the topographic effect of the Laurentide
106 ice sheet, and slowdowns on the Atlantic Meridional Overturning circulation (AMOC). Thus,
107 the westerly jet gives us a way to connect paleoclimate influences to specific changes in the East
108 Asian rainfall climate.

109 The role of the westerly jet and jet transitions in East Asian paleoclimate is an emerging
110 hypothesis. The westerlies features prominently in how the rise of Tibetan Plateau over the last
111 several million years altered Asian climate; *Molnar et al.* [2010] provides a summary and
112 perspective on these ideas, and also speculate on the role of the westerly jet in the more recent
113 paleoclimate changes. However, the first and most comprehensive exposition (to the authors'
114 knowledge) of the role of jet transitions during the last glacial period and Holocene was
115 advanced by Kana Nagashima and colleagues [*Nagashima et al.*, 2007; *Nagashima et al.*, 2011],
116 Nagashima and Tada, 2012], who hypothesized a delayed seasonal jet transition from south of
117 Tibet to the North during D/O stadials. They proposed this hypothesis specifically to explain
118 their dust flux record from an ocean sediment core in the Sea of Japan, and drew on
119 contemporary understanding of westerly jet dynamics in formulating their hypothesis. While we
120 follow similar motivations as with Nagashima and colleagues in formulating our hypothesis, we

121 expand the hypothesis by exploring the ramifications of the hypothesis in particular to the
122 atmospheric circulation dynamics and oxygen isotopic changes in rainfall. We also present
123 initial modeling evidence supporting this hypothesis, as well as presenting a modern-day analog
124 that illustrates in detail the nature of a delayed jet transition on the climate of East Asia and
125 surroundings.

126 We first summarize what is known regarding the East Asian seasonal transitions, and their
127 relationship to the seasonal jet transition (section 2). We then advance a specific hypothesis (the
128 ‘Jet Transition’ hypothesis) for East Asian paleoclimate changes, and discuss the predictions of
129 the hypothesis (section 3). In section 4, we show observational evidence that the meridional
130 position of the westerly jet is tied to modulation of the timing of seasonal transitions in today’s
131 East Asian monsoon variability. Following this, we explore our hypothesis with model
132 simulations of two paleoclimate scenarios, North Atlantic cooling and orbital variations
133 (precession), showing the viability of the hypothesis (section 5). We then explore how the
134 hypothesis can be made consistent with speleothem $\delta^{18}\text{O}$ records (section 6), and also discuss
135 how the hypothesis may be consistent with other key paleorecords, including dust (section 7).
136 We end with discussion and conclusions (section 8).

137 2. Background

138 *Ding and Chan* [2005] noted in an influential review paper on East Asian monsoon that the
139 “seasonal march of the East Asian summer monsoon displays a distinct stepwise northward and
140 northeastward advance, with two abrupt northward jumps and three stationary periods”. **Figure**
141 **2** (modified from *Ding and Chan 2005*) summarizes the evolution: starting from persistent
142 rainfall in Spring, the ‘pre-Meiyu’ phase starts in early May with the start of rainfall surges over
143 the South China Sea; rainfall over Southern China also intensifies. Meiyu rainfall starts

144 sometime in the first half of June, when the preferred latitude of rainfall shifts rapidly northward
145 to central China along the valley of the Yangze River. This second quasi-stationary stage
146 persists for 20-30 days until another shift occurs during early-mid July, when rainfall jumps well
147 north ($\sim 35^{\circ}\text{N}$), ending the Meiyu stage. This Summer rainfall then occurs over northern China,
148 whereas central and southern China ($\sim 24^{\circ}\text{N}$ to $\sim 35^{\circ}\text{N}$) becomes relatively dry. (NOTE: our
149 references to **Spring, Pre-Meiyu, Meiyu, and Summer**, first letter in capital, will specifically
150 refer to the dynamical stages of rainfall). These complex stages contrast with other monsoon
151 systems that tend to have a simpler evolution. For example, the West African and South Asian
152 summer monsoon rainfall evolves fairly smoothly after the abrupt onset in early summer, until its
153 termination in September (**figure 3**). It suggests that other factors, not typical of monsoons,
154 influence East Asia.

155 One crucial feature that is not shared by other monsoons is that the East Asian monsoon
156 penetrates the midlatitudes ($\sim 42^{\circ}\text{N}$), well into the latitudes of the upper-level westerlies.
157 Moreover, the Tibetan Plateau has a pronounced effect on the configuration of the westerlies
158 over East Asia. In the absence of the Plateau, the westerlies flow zonally, unimpeded by the
159 topography. In the presence of the Tibetan Plateau however, the westerlies flow around to the
160 south or north of the Plateau, depending on the latitude of the westerlies impinging upstream of
161 the Plateau [*Schiemann et al.*, 2009]. In the Spring month of April and prior, the jet is located
162 south of the Plateau (**figure 4**). In May the jet transitions northward over Tibet until June when
163 the jet sits north of Tibet, hugging the northern boundary. In July, the jet extends further
164 northwards away from the northern boundary of Tibet [*Lin and Lu 2008*].

165 The Chinese monsoon literature has long noted that the rainfall transitions are timed to

166 the seasonal evolution in latitudinal position of the westerly jet impinging on the Tibetan Plateau.
167 The first directed studies published in English are those by *Academia Sinica [1957, 1958a,b]* and
168 *Yeh et al. [1959]*, and subsequent studies have since provided compelling evidence of this
169 association (e.g. *Liang and Wang, 1998; Schiemann et al., 2009*). When the jet is south of Tibet,
170 East Asia experiences Spring rains. The transition of the jet to the north of the Plateau marks
171 the start of the Pre-Meiyu, and the Meiyu front (and associated rainfall) across central China
172 forms once the jet has fully transitioned to the North. A weakening of the jet and further
173 northward displacement occurs in July, timed with the disappearance of the Meiyu front and the
174 jump of rainfall to North China. In short, the distinct phases of seasonal rainfall - Spring, pre-
175 Meiyu, Meiyu, and Summer – are tied to the meridional transitions (relative to the Plateau)
176 during the northward evolution of the westerly jet.

177 Recent dynamical work suggests that changes in meridional jet position *cause* the
178 seasonal transitions in the East Asian rainfall. During the spring when the jet is South of the
179 Plateau, the resulting downstream circulation experiences dynamical large-scale uplift that leads
180 to a relatively weak but persistent rainfall across southeastern China. The ‘Spring Persistent
181 Rains’ are well known (e.g. *Wu et al., 2007*), and quite distinct from the convective rainfall
182 associated with the East Asian summer monsoon. The mechanisms of the large-scale uplift
183 downstream of Tibet are still being investigated, but it has been simulated in AGCM simulations
184 where the Tibetan highlands is gradually introduced [*Chen and Bordoni, 2014; Park et al., 2012;*
185 *Wu et al., 2007*] and in more idealized simulations with a dry atmospheric model with an
186 idealized imposed mountain [*Molnar et al., 2010; Park et al., 2012*]. Observational analysis of
187 the moist static energy budget and AGCM experiments indicate that the interaction between the
188 jet and the Tibetan plateau causes anomalous advection of dry enthalpy into the Meiyu region,

189 and that this advection plays an important role in maintaining the Meiyu front [*Chen and*
190 *Bordoni, 2014*].

191 On the other hand, the Meiyu front arises from the circulation downstream of Tibet when the
192 jet flows around its northern edge; the jet separates the warm moist air over South China from
193 the dry cooler air to the north, and transient eddies carried by the jet along the front bring about
194 frontal convection that is the hallmark of Meiyu rainfall [*Ding and Chan, 2005; Sampe and Xie,*
195 *2010*]. In addition, advection warm air by the westerlies from the eastern flank of the Tibetan
196 Plateau induce upward motion over the Meiyu front latitudes, promoting convection over that
197 region [*Sampe and Xie, 2010*]. Finally, when the jet maximum systematically shifts northwards
198 away from the Tibetan Plateau and weakens, these effects and thus the Meiyu front disappears.
199 As a result, monsoonal flows are able to transport moisture to the northern reaches of China
200 (north of 35°N) where they undergo convection. The northward shift of the jet co-incident with
201 the onset of the Western North Pacific summer monsoon [e.g. *Ueda et al. 2009*] and the resulting
202 atmospheric dynamical adjustment from the diabatic heating is thought to contribute to the jet
203 shift.

204 **3. Seasonality and the Jet Transition Hypothesis**

205 We seek to incorporate the complex rainfall seasonality of East Asia into the interpretation of
206 East Asian paleoclimate. In order to do this, we focus on the quasi-stationary stages and
207 transitions in the East Asian rainfall seasonality, and the role of the westerlies as the determinant
208 of these stages. At a gross level, the position and strength of the westerlies are tied to changes in
209 the meridional temperature gradient through thermal wind [e.g. *Holton, 2004*]; as such, many
210 paleoclimate forcings are well suited to altering the westerlies. For example, both the
211 Dansgaard-Oeschger (D/O) cycles and precessional changes readily alter the equator-to-pole

212 temperature gradient. D/O stadials are characterized by intense North Atlantic cooling that cools
213 the entire northern hemisphere, weighted towards the higher latitudes; and the low NH summer
214 insolation phase of precession cools the entire Northern Hemisphere during the summer, also
215 weighted towards the higher latitudes (we will show simulated jet changes in the next section).
216 Atmospheric teleconnections resulting from convection changes in the Tropics can also lead to
217 changes in the westerlies impinging over Tibet; for example, an earlier or later onset of the
218 Western North Pacific summer monsoon may result in changes in the northward shift of the
219 westerlies in mid-July, similar to what is seen in the interannual variations of the ‘Pacific-Japan’
220 teleconnection pattern [*Hsu and Lin 2007; Kosaka and Nakamura 2010*].

221 We posit that the meridional variation of the westerly jet impinging on the Tibetan
222 Plateau is key to interpreting paleoclimate change. As such, we propose this hypothesis:
223 ***Jet Transition Hypothesis:*** *changes to the seasonal meridional position of the westerlies relative*
224 *to the Tibetan Plateau drive rainfall climate changes over East Asia on paleoclimate timescales.*

225 A schematic of the East Asian seasonal cycle (**figure 5**) qualitatively illustrates this
226 hypothesis and its predictions. Here, the y-axis is an idealized measure of the seasonality, which
227 in our hypothesis is linked to the meridional position of the westerlies relative to the Plateau.
228 The various stages of East Asian rainfall seasonality – Spring, pre-Meiyu (jet transition), Meiyu,
229 and Summer - are marked in the schematic. The ‘normal’ seasonal cycle (solid black line)
230 undergoes the usual seasonal Spring-Meiyu-Summer rainfall transitions. In scenario A (red
231 dashed line) with the jet extending further North at its peak, the main effect is a longer Summer
232 regime, associated with an earlier South-to-North transition and/or a shortened Meiyu. In
233 scenario B (cyan dashed line), the South-to-North transition occurs later; the main feature is that
234 there is no transition to Summer; rather, it persists in the Meiyu. In an extreme scenario C

235 (dashed blue line), the jet does not transition to the North, and the East Asia rainfall regime stays
236 largely in either Spring or Winter.

237 While the hypothesis is crude and qualitative as currently stated, it offers predictive tests that
238 can be used to explore and subsequently refine the hypothesis. We do so in section 5 with some
239 model simulations.

240 **4. Modern-day interannual analog of seasonal transitions**

241 Before we explore paleoclimate scenarios with models however, we use the modern-day
242 variability of the East Asian monsoon to illustrate the climate and circulation changes associated
243 with the timing of the seasonal transitions, taking advantage of observational and reanalyses
244 datasets. By showing that modern analogs exist, it lends credibility to the Jet Transition
245 hypothesis. We specifically examine the variability of the Meiyu onset, and the variability in the
246 Meiyu-to-Summer transition.

247 *4.1 Variability in the Meiyu onset*

248 The Meiyu onset occurs during mid-June (see **figure 2**) [*Ding and Chan, 2005*] but there
249 is year-to-year variability about that onset date. This variability and its association with the
250 westerly jet is captured in a maximum covariance analysis (MCA; *Bretherton et al., 1992*) of
251 June mean upper tropospheric zonal winds averaged over 500-100mb (left field) and
252 precipitation (right field) (**figure 6**). We used NCEP reanalysis [*Kalnay et al., 1996*] for the
253 zonal winds, and Global Precipitation Climatology Center (GPCC) gridded station rainfall
254 [*Schneider et al., 2008*]. The zonal wind domain (50-130°E, 20°N-50°N) used for the MCA is
255 taken over the span of the Tibetan Plateau as well as upstream and downstream regions. The
256 precipitation domain is taken over the East Asian summer monsoon region (105-123°E, 21-
257 40°N). We apply the MCA over the full period of overlap between the two datasets (1958-

258 2010); prior to the MCA, both precipitation and zonal wind are normalized at each gridpoint.
259 There are documented issues with discontinuities in the NCEP reanalysis, in particular with the
260 incorporation of satellite information post-1979; in order to verify our result, we also did the
261 same analysis over the period 1979-2010; the results were essentially the same. We also repeated
262 the MCA using the newer but shorter NCEP2 reanalyses [*Kanamitsu et al.*, 2002] over 1979-
263 2010; similar results were obtained (not shown).

264 The method essentially extracts the variation in the Meiyu onset as the first mode,
265 associated with north-south displacement in the westerly jet strength; mode 1 explains around
266 56% of the squared covariance fraction. The spatial pattern of the first mode shows stronger
267 upper-tropospheric zonal winds to the north and weaker to the south associated with stronger
268 precipitation over northern China and weaker over Southern China (**figure 6a**). The
269 corresponding zonal wind expansion coefficient timeseries (**figure 6b**) shows interannual
270 variability but no noticeable trend for the time period of analysis; the precipitation expansion
271 coefficient (**figure 6c**) likewise display pronounced interannual variations correlated to the zonal
272 expansion coefficients, but also suggest multidecadal variation with low values prior to the late
273 1970's and after the late 1990's, and higher values between the two periods.

274 We seek confirmation that MCA mode 1 is associated with the timing of northward jet
275 transition. We use an occurrence-based jet climatology data developed by *Schiemann et al.*
276 [2009] to do composites of meridional median jet latitude from 90°E - 130°E for 'high' and
277 'low' years of the mode 1 U wind expansion coefficients (**figure 7a-c**). This data essentially
278 counts the occurrence of local jet maxima in the 3-dimensional wind field using the 40-year
279 ECMWF reanalyses (ERA-40; *Uppala et al.*, 2005) at 6-hourly intervals over 1958-2001 (see
280 *Schiemann et al.* [2009] for details). The Jet occurrence data between June 11-20 of 'high' years

281 **(figure 7a)** – corresponding to a more northward mean zonal wind in the MCA – occupies a
282 stretch of longitudes across East Asia between 35°N and 40°N (and with a slight northeast to
283 southwest tilt). ‘Low years’ **(figure 7b)** shows a slightly more southward distribution of jet
284 occurrences than those for ‘high’ years **(figure 7c)**, consistent with a delayed northward
285 transition for ‘low’ years.

286 We use this interannual analog to gain insight into the regional climate changes of a
287 varying jet transition by regressing the U expansion coefficients against various monthly fields
288 of interest. With an earlier onset to the Meiyu, low-level southerlies increase over East Asia
289 **(figure 8a)**, bringing moisture further inland and shifting convection northwards **(figure 8a and**
290 **9a)**. Low-level moist static energy increases over the Meiyu front latitudes of 30-35°N **(figure**
291 **8b)**. The regression pattern onto June precipitation over the larger Asian region demonstrates
292 the influence of the westerlies on the precipitation pattern **(figure 9a, shaded)**. The effect of an
293 earlier northward transition is evident – less rainfall over China south of ~30°N, and more to the
294 north of it; increased rainfall also occurs over the Korean peninsula and southern Japan.
295 Intriguingly, there is also increased rainfall over northeastern India associated with this MCA
296 pattern, suggesting that there may be some connection to rainfall there as well.

297 4.2 *Variability in the Meiyu-to-Summer transition*

298 We repeat the same MCA analysis as in section 4.1, but using July-August averaged fields to
299 capture the variation in the Meiyu-to-Summer transition. From previous studies, we expect there
300 to be significant interannual variation in the westerlies, and associated with July-August rainfall
301 changes over East Asia [e.g. *Lin and Lu 2008, Kosaka et al. 2011*]; in particular, *Kosaka et al.*
302 *(2011)* also used MCA to extract a relationship between the Meiyu-Baiyu rainfall anomalies and
303 thermal advection by the westerlies, and they invoked the mechanism by *Sampe and Xie (2010)*

304 to account for the linkage. Results are shown in **figure 10**. As with the June analysis, the
305 dominant pattern (explaining around 56% of the squared covariance fraction) is a north-south
306 dipole in the zonal wind field with increased westerlies to the north associated with a ‘tripole’
307 pattern in precipitation with positive values over northern China, negative values over the Meiyu
308 front latitudes, and positive again over southern China (also see **figure 9b**). Composites of the
309 jet count data (similar to what was done in section 4.1 with the June MCA mode 1) confirm that
310 this pattern is associated with an earlier jet transition to the north (**figure 7d-f**). Moreover,
311 associated low-level winds, vertical velocity, and 925mb moist static energy changes (**figure**
312 **8c,d**) suggest increased moisture transport penetrating north of the Meiyu front, resulting in
313 convection over Northern China. The pattern is consistent with the interpretation that an earlier
314 northward transition of the westerly jet in this season is linked to an earlier Meiyu-to-Summer
315 transition.

316 The associated precipitation pattern over East Asia for this MCA mode 1 (**figure 9b**)
317 bears close resemblance to a well-known ‘tripole’ pattern in East Asian rainfall anomalies
318 [*Chang et al.*, 2000; *Hsu and Liu*, 2003; *Weng et al.*, 1999]; for example, *Hsu and Lin* [2007]
319 showed that it arises as the first EOF of detrended June-August averaged rainfall over 1962-97.
320 Interestingly, they show that this extracted precipitation pattern is tied to a meridional shift in the
321 mean westerly jet axis across the whole of Asia (see figure 11 of *Hsu and Lin* 2007). To further
322 compare our results to *Hsu and Lin* [2007], we regressed the zonal wind expansion coefficients
323 for the Jul-Aug MCA mode 1 to July-Aug 100-500mb averaged zonal winds (**figure 9b**
324 contours). The regression clearly indicates the elongated pattern of westerly changes stretches
325 from the Near East across Asia and into the Western North Pacific, similar to what was found in
326 *Hsu and Lin* [2007]. For completeness, we performed a similar regression of June mean upper

327 tropospheric westerlies onto the June MCA1 U expansion coefficients (**figure 9a**, contours).
328 The results are similar to that found for the July-August case, showing again that an earlier
329 (later) transition is linked to northward (southward) displacement in the westerly jet axis.

330 The underlying dynamics of this ‘precipitation tripole’ remains to be elucidated, though *Hsu*
331 *and Lin* [2007] show that the interannual variability of their precipitation tripole is forced by a
332 number of factors, including the tropical Pacific, disturbances from the extratropics, as well as
333 changes to heating over the eastern Tibetan Plateau. It led them to speculate on the intrinsic
334 nature of this mode of behavior, that the “tripole pattern is a result of the amplification of an
335 intrinsic dynamic mode that can be triggered by various factors despite their different origins”.
336 This interpretation, if true, would support to our hypothesis that the westerly jet is sensitive to
337 north-south perturbations, and that it leads to significant precipitation variations across East Asia.

338 Finally, we note in passing that the extracted July-August MCA mode 1 exhibits an
339 intriguing trend over the period of analysis in both expansion coefficients, and suggesting a later
340 Meiyu-to-Summer transition from the mid-to-late 20th century (**figure 10b,c**). In fact, the
341 precipitation trends resembles the well-known ‘North-Drought, South Flood’ pattern observed
342 over the latter half of the 20th century [*Hu et al.*, 2003; *Xu*, 2001; *Zhou et al.*, 2009], where
343 summer precipitation underwent a wetting trend over central China but a drying trend in the
344 north (note that *Hsu and Lin* [2007] detrended their precipitation data prior to analysis, but did
345 acknowledge the existence of a significant trend in the tripole pattern). *Yu et al.* [2004] linked
346 this “North-Drought, South Flood” pattern to a tropospheric cooling trend over East Asia that,
347 according to them, led to a southward shift of the tropospheric westerlies. However, whether or
348 not our extracted July-August MCA mode 1 pattern is indeed linked to the ‘North-Drought,
349 South Flood’ pattern requires further study; in particular, this pattern will have to be reproduced

350 with independent observational data (given the limitations in NCEP reanalysis regarding long-
351 term trends), and dynamical reasons will have to be found for why and how this trend occurred.

352 **5. Exploring the hypothesis with model simulations**

353 We now explore our hypothesis using paleoclimate simulations of the higher-resolution
354 $0.9^\circ \times 1.25^\circ$ (lat/lon) version of the Community Atmosphere Model version 5 (CAM5) [Neale *et*
355 *al.*, 2010]. The version we use is coupled to a 50m thermodynamic ‘slab’ ocean, so that
356 thermodynamic ocean-atmosphere feedbacks – especially important for the tropics - are
357 incorporated. This model has an excellent simulation of the East Asian seasonal rainfall climate
358 (**figure 11a**), showing the separation into Spring, Meiyu, and Summer rains, and serves as an
359 ideal platform to explore some of our ideas.

360 *5.1 Precession*

361 Years of modeling research, starting with the pioneering work by *Kutzbach* [1981] have shown
362 that northern hemisphere monsoons respond strongly to precessional insolation forcing. The
363 East Asian monsoon climate is no exception, and speleothem records show large and abrupt
364 variations timed to precessional cycles. The conventional interpretation calls for more intense
365 summer monsoons during times when northern hemisphere summer insolation is high [*Wang et*
366 *al.*, 2008]; the northern hemisphere (and in particular the high latitudes) will be warmer than
367 today, and the equator-to-pole temperature gradient should weaken at least in the summer
368 months. Thus, the prediction would be for a more northerly-positioned jet and an early transition
369 into the Meiyu and Summer rainfall regimes.

370 We use orbital conditions from 11,000 years ago corresponding to a time when northern
371 summer insolation was close to its precessional peak. When these orbital conditions are applied
372 to CAM5, keeping all other boundary conditions fixed to present-day, the model’s rainfall

373 responds with an earlier transition to the Meiyu, and to Summer rainfall (**figure 11b and c**); the
374 model simulation also stays in Summer rainfall conditions longer until the transition to Fall
375 conditions. All of these are in broad accordance with the proposed hypothesis (scenario ‘A’ in
376 figure 5).

377 The westerly jet over East Asia shows an apparent early transition to the North. Top-of-
378 atmosphere (TOA) insolation increases (relative to today) over the Northern hemisphere Tropics
379 and midlatitudes from mid-April through early September, peaking in June and July with a
380 $\sim 40\text{Wm}^{-2}$ increase (**figure 12**). We expect a similar timing in the changes to the westerlies over
381 Asia. **Figure 13a** shows the June-August zonal wind changes averaged over East Asia (100°E -
382 125°E). They show reduced zonal westerlies in the southern part of the mean westerlies, which
383 we interpret to mean an earlier northward transition of the jet. The anomalies appear from mid-
384 April through mid September and peak in early July (not shown), roughly coincident with the
385 timing of the insolation anomalies.

386 5.2 *North Atlantic Cooling*

387 In this second test case, we apply a 45W/m^2 SST cooling in the extratropical North Atlantic to an
388 atmospheric general circulation model coupled to a slab ocean (similar to what was done in
389 *Cvijanovic and Chiang* [2013], but with a newer model and higher resolution). North Atlantic
390 cooling is associated with Dansgaard-Oeschger (D/O) stadials, which are in one-to-one
391 correspondence with Chinese speleothem records (e.g. *Wang et al.*, 2001). However, our run is
392 embedded in a present day basic state; as such, our simulation would be more analogous to the
393 8.2ka North Atlantic cold event during the Holocene when the basic state climate (continental ice
394 sheet, sea level, and greenhouse gas distributions) was more similar to modern. This event’s

395 impacts included dry conditions over East Asia according to Chinese speleothem records [*Cheng*
396 *et al.*, 2009a; *Liu et al.*, 2013].

397 The results are not as clear-cut as for the precessional run, but do show a delay in the Spring-
398 to-Meiyu transition, as well as the Meiyu-to-Summer transition (**figure 14**). The duration of
399 Summer rains is also shorter. Moreover, the summer westerlies appear to be weakened over the
400 mean westerly maximum, and strengthened to the south of it, suggesting a mean southward shift
401 of the westerly jet axis (**figure 13b**). This interpretation is not clear-cut, as there is also an
402 increase (albeit weaker) in the westerlies to the north of the jet; however, given that the
403 anomalous westerlies are larger over the southern lobe and closer to jet maximum, we interpret
404 this to mean that the South to North transition of the westerly jet across the Plateau was delayed,
405 consistent with the behavior of rainfall.

406 The relative lack of response in the westerlies over East Asia to North Atlantic cooling, at
407 least for the CAM5, points to a potential weakness in our hypothesis. However, when we
408 applied a similar North Atlantic cooling to another model (the Community Atmosphere Model
409 version 3 at T42 resolution), the southward displacement of the westerlies over East Asia was
410 clearer and more pronounced (not shown). Thus, it is likely that the magnitude of the response is
411 model-dependent, and possibly from different strengths in radiative feedbacks: *Liu et al.*
412 (2014) found that the downstream cooling resulting from North Atlantic cold forcing was
413 amplified by positive feedbacks, in particular water vapor and clouds. To advance this
414 hypothesis, more needs to be done to understand the teleconnection between North Atlantic
415 cooling and westerlies over East Asia.

416 6. Explaining Cave Speleothem $\delta^{18}\text{O}$ records

417 We now show how the hypothesis produces a viable explanation for changes to the East Asian
418 speleothem $\delta^{18}\text{O}$ records, by considering the modern-day seasonal cycle in the $\delta^{18}\text{O}$ of
419 precipitation and how it is linked to the seasonality of East Asian rainfall and jets. The ideas
420 here closely parallel the summer/non-summer rainfall ratio ideas introduced by *Wang et al.*
421 *[2001]* and *Cheng et al. [2009]*, but using the observed monthly climatology of precipitation
422 $\delta^{18}\text{O}$ to quantify the potential changes across East Asia.

423 6.1 Seasonal cycle of precipitation $\delta^{18}\text{O}$

424 Measured isotopes from various stations in East and South China show a gross seasonal cycle in
425 the $\delta^{18}\text{O}$ of precipitation (hereafter $\delta^{18}\text{O}_p$) with heavier isotopes in winter and lighter isotopes in
426 summer. **Figure 15**, taken from *Dayem et al. [2010]*, nicely summarizes these observations. In
427 general, for stations south of the Meiyu front, there is a general pattern with relatively heavy
428 $\delta^{18}\text{O}$ during the winter, and lighter during the summer. However, there is also a variation to this
429 seasonality, with southeastern stations (Liuzhou, Guilin, Hong Kong) shifting to lighter isotopes
430 earlier in the season (May) than the northern and western stations (Nanjing, Zunyi, Guiyang,
431 Kunming), which shift in June.

432 This variation in seasonality is succinctly shown with a combined empirical orthogonal
433 function (CEOF) analysis of the seasonal cycle in $\delta^{18}\text{O}_p$ over GNIP stations in China (south of
434 36°S and east of 100°E , and below 2000m elevation) (**figure 16** – see caption for details).
435 EOF1 (**figure 16, left column**) is the seasonal cycle associated with the summer/winter
436 monsoon: more rain in summer and less in winter, and lighter $\delta^{18}\text{O}_p$ in the summer (south of
437 35°N). EOF2 (**figure 16, right column**), on the other hand, is associated with springtime
438 changes: the principal component (PC) loadings are large and positive in April and May but
439 small and negative in other months; and the spatial loading show differences in the properties

440 between southeastern China (with large positive precipitation loadings and small but positive
441 $\delta^{18}\text{O}_p$ loadings) compared to those over central China (small positive precipitation loadings and
442 large positive $\delta^{18}\text{O}_p$ loadings). As will be elaborated in section 6.2, mode 2 reflects the
443 difference in *timing* of convective monsoon onset, earlier over Southern China and later over
444 Central China; and associated with it, changes in the $\delta^{18}\text{O}_p$.

445 6.2 Interpretation of seasonal $\delta^{18}\text{O}_p$

446 We argue that this spring modulation in precipitation and $\delta^{18}\text{O}_p$ (as reflected by EOF mode 2)
447 has a straightforward physical interpretation derived from the relationship between jet position
448 and the various stages in East Asian rainfall. It reflects two physical properties: (i) moisture
449 associated with low-level monsoonal flow from the south is isotopically light, and also
450 associated with more rainfall; and (ii) the latitudinal position of the westerly jet limits the
451 northward penetration of monsoonal low-level moisture transport. Moisture associated with low-
452 level monsoonal inflow is isotopically light because precipitation upstream of East Asia –
453 namely over the Indian ocean and South China Sea –preferentially removes the heavier isotopes
454 from the water vapor being transported to land (the so-called ‘rainout effect’ [*Dansgaard,*
455 1964]).

456 The second property allows us to tie the spatial properties of EOF2 - for both
457 precipitation and $\delta^{18}\text{O}_p$ - to the known jet and precipitation seasonality. During April and May,
458 the jet position is either south or over the Plateau and low-level monsoonal inflow from the south
459 penetrates only into southernmost China; thus $\delta^{18}\text{O}_p$ starts becoming lighter and rainfall increases
460 only for the southernmost regions of China in Spring. On the other hand, central and northern
461 China lacks the low-level monsoonal moisture from the south during this time, so the
462 precipitation is small and $\delta^{18}\text{O}_p$ is heavy. *This pattern is essentially what is captured in EOF2.*

463 With the Meiyu onset in June, the jet shifts north and low-level monsoonal moisture is able to
464 penetrate to the northern limit of the Meiyu front ($\sim 35^\circ\text{N}$); and finally with the onset of Summer
465 rains and disappearance of the Meiyu front, the low-level moisture is able to penetrate north of
466 35°N .

467 Individual station precipitation and $\delta^{18}\text{O}_p$ seasonal cycles (**figure 15**) demonstrate the
468 spatial difference in the timing of convective monsoonal onset and its influence on $\delta^{18}\text{O}_p$. For
469 example, in the southeastern Chinese city of Guilin (25°N 110°E), the rainfall increases and
470 $\delta^{18}\text{O}_p$ decreases sharply between April and May, indicating a May onset; whereas further north in
471 Nanjing (32°N 118°E), the onset is shifted to June.

472 Moisture transport fields in NCEP reanalysis support the above interpretation. We
473 regress the PCs of the EOFs onto 925mb climatological total moisture transport and moisture to
474 show the lower tropospheric moisture transports and moisture content associated with each EOF
475 (**figure 17**). The results indicate that while EOF1 is associated with lower tropospheric
476 monsoonal moisture transport from the south penetrating well into Northern China (**figure 17a**),
477 moisture transport associated with EOF2 is limited to South and Central China (**figure 17b**).

478 6.3 *The Jet Transition hypothesis and speleothem $\delta^{18}\text{O}$*

479 We now explore how a modified jet seasonal cycle may impact $\delta^{18}\text{O}_p$, given our interpretation
480 above. Consider the extreme situation where the jet remains South of the Plateau virtually all
481 year (scenario C in fig5), and rainfall stays ‘stuck’ in the Spring regime. What would this do to
482 the $\delta^{18}\text{O}_p$ of annual mean rainfall?

483 Returning to the results of our combined EOF analysis, we artificially apply the
484 prolonged Spring conditions by setting the PC 1 and 2 loadings for May through October - the
485 months when the jet is either transitioning or to the north of the Plateau – to the average of the

486 April and May PC values (**figure 16a and d, dashed lines**). The monthly climatological
487 precipitation and $\delta^{18}\text{O}_p$ at each station is then reconstructed from the modified PC1 and 2
488 loadings. **Figure 18** illustrates how precipitation and $\delta^{18}\text{O}_p$ is altered. For the example of
489 Nanjing (the station closest to Hulu cave), climatological precipitation is slightly reduced in the
490 summer (**figure 18a, dashed lines**), but the main effect is the heavier $\delta^{18}\text{O}_p$ for the summer
491 months (**figure 18b, dashed lines**). Across the various stations over China, total precipitation
492 does change but not in a systematic fashion – some stations (primarily over southern China)
493 increase, but most others decrease typically by 20%. The more striking feature is that the
494 precipitation-weighted annual mean $\delta^{18}\text{O}_p$ is heavier throughout, in particular for stations away
495 from southeastern China. For Nanjing, the increase in the precipitation-weighted annual mean
496 $\delta^{18}\text{O}_p$ is +2.45 per mil.

497 How do these values compare to the speleothem record? If we decompose the Wang et
498 al. (2008) speleothem $\delta^{18}\text{O}$ record – which combines records from Hulu cave (32°30'N,
499 119°10'E) and Sanbao cave (31°41'N, 110°27'E) (**figure 18** plots their locations) - into its
500 millennial, precessional, and glacial-interglacial components using Ensemble Empirical Mode
501 Decomposition [*Wu and Huang, 2004*] (**figure 19**), the amplitude of variations are ~2 per mil,
502 ~3-4 per mil, and ~1 per mil respectively. Thus, our hypothesis appears plausible for explaining
503 millennial variations in the $\delta^{18}\text{O}_p$ record, as well as glacial-interglacial variations, though it is
504 unable to explain the entirety of the precessional signal.

505 6.4 Comparison with other interpretations of speleothem $\delta^{18}\text{O}$

506 Associating $\delta^{18}\text{O}$ variations to precipitation intensity dominates current interpretations of
507 speleothem oxygen isotope records. However, several recent studies [*Pausata et al., 2011; Yuan*
508 *et al., 2004; Lee et al., 2012*] have proposed an alternative hypothesis that the speleothem $\delta^{18}\text{O}$

509 represent the strength of precipitation occurring upstream from East Asia, and not of rainfall over
510 East Asia itself; if precipitation increases upstream of East Asia, the resulting moisture
511 transported to the continent becomes isotopically lighter, and this becomes reflected in the East
512 Asian precipitation $\delta^{18}\text{O}$. At face value, the upstream interpretation does not require climate and
513 rainfall changes over East Asia, though it does not exclude them either.

514 A compelling part of the ‘upstream’ argument is that it predicts $\delta^{18}\text{O}$ variations to be
515 spatially coherent across large regions. This is indeed observed in the spectrum of East Asian
516 speleothem records: the Hulu, Sanbao and Dongge cave records show $\delta^{18}\text{O}$ variations that
517 virtually track each other in shape and magnitude in the periods of overlap [*Wang et al.*, 2008].
518 On the other hand, the ‘intensity’ interpretation struggles to explain this spatial coherence, as
519 observations of precipitation $\delta^{18}\text{O}$ do not suggest a large spatial coherence: the correlation
520 between precipitation amount and $\delta^{18}\text{O}_p$ at any given station is weak, nor is there a large-scale
521 coherence in rainfall amount changes over East Asia [*Dayem et al.*, 2010].

522 Our hypothesis also predicts a broad spatial coherence of the $\delta^{18}\text{O}$ signal across, but
523 differently from the upstream hypothesis. In our case, the broad coherence is a direct
524 consequence of the large-scale nature of the East Asian seasonal circulation and its changes.
525 There are, however, predicted differences in *magnitude* of the $\delta^{18}\text{O}$ response: from **figure 18d**,
526 smaller $\delta^{18}\text{O}_p$ responses are seen over the southeastern coastal China, but increases as one moves
527 northwards and westwards; the largest changes are seen over southwestern China near the
528 foothills of the Tibetan Plateau. A cursory visual comparison of the predicted changes to the
529 cave locations in **figure 18d** suggest that $\delta^{18}\text{O}$ changes at Hulu and Sanbao caves would be of
530 similar magnitude; whereas Dongge cave may undergo slightly smaller changes, and
531 Xiaobailong cave would experience significantly larger changes than for the other caves. A

532 recent long speleothem $\delta^{18}\text{O}$ record from Xiaobailong indeed appears to show larger amplitude
533 variations in particular for precessional cycles [*Cai et al.*, in preparation]. A more quantitative
534 comparison, however, will have to wait for the advent of climate models that accurately
535 represent both water isotopes and seasonality of rainfall over East Asia.

536 A recent study by *Liu et al.* [2014] attempted to reconcile the intensity and upstream
537 interpretations. They found – based on results of a coupled model simulation of the last 21,000
538 years and explicitly modeling water isotopes – that the upstream depletion has significant control
539 of modeled $\delta^{18}\text{O}_p$ variations over China. However, they also found that isotopic variations in
540 East Asian precipitation are associated with modeled precipitation changes over China, and
541 closely correlated to the strength of the southerly East Asian monsoon inflow. They suggest
542 from these results that speleothem $\delta^{18}\text{O}$ is indeed a robust indicator of East Asian monsoon
543 changes (and in particular the southerly monsoonal inflow), even with significant control of
544 $\delta^{18}\text{O}_p$ by upstream variations. They argue that this occurs because of the large-scale coherence
545 of Northern Hemisphere monsoon variations in controlling both convection over East Asia and
546 upstream of it.

547 Our hypothesis is not inconsistent with, and appears complementary to, the interpretation
548 offered by *Liu et al.* [2014]. A stronger southerly monsoonal flow may be indicative of an
549 earlier onset of the Meiyu and/or Summer rainfall; we note that an earlier onset of either would
550 be marked by stronger monsoon southerlies, as found in our interannual analogs (see **figure 8**).
551 We note that the simulations in *Liu et al.* [2014] were done in coarse resolution (T31, or roughly
552 3.75° resolution), likely too coarse to accurately simulate the Spring/Meiyu/Summer seasonal
553 regimes or the transitions between them; we note, however, that in the simulations of *Liu et al.*
554 [2014], lighter modeled $\delta^{18}\text{O}_p$ over China is associated with increased rainfall over northern

555 China and reduced rainfall over central China, resembling an earlier Meiyu-to-Summer transition
556 (cf **figure 9b**).

557 In practice, it is likely that all of the factors discussed – intensity, seasonality, and
558 upstream effect – play a role in the observed East Asian speleothem $\delta^{18}\text{O}$ variations. Our
559 hypothesis alone would struggle to explain the magnitude of the ~3-4 per mil precessional
560 variations in the speleothem record (**figure 19**), but a combination of factors may be able to
561 account for the changes. Interestingly, precessional changes in the earlier half (earlier than
562 110,000 ybp) of the *Wang et al.* [2008] $\delta^{18}\text{O}$ record show a relatively smooth variation during the
563 extrema of precessional insolation phases, but also exhibit abrupt transitions from one extremum
564 to the other (see figure 1); this suggests that different dynamics are at play for the two behaviors.
565 Could the smoothly varying portion be related to upstream variations, whereas the abrupt portion
566 tied to the westerly jet shift?

567 7. Comparison to other East Asian paleoclimate records

568 In this section, we review other paleoevidence to support the interpretation that East Asian
569 paleoclimate change can be viewed as a modulation of seasonality, driven by meridional
570 displacement of the westerly jet seasonal cycle relative to present day. This distinguishes our
571 hypothesis from the ‘intensity’ and ‘upstream’ interpretations mentioned previously. There are
572 at least two features of the East Asian paleoclimate evidence that our hypothesis may explain
573 that are not readily explainable by either the intensity or upstream interpretations, namely: (i)
574 changes in dustiness and dust transport in East Asia, and (ii) the spatial variation in the timing of
575 the Holocene precipitation peak. We elaborate each of these, below.

576 7.1 *Dust records*

577 It is clear from proxy dust records that the East Asian climate is dustier during cold North
578 Atlantic events. The westerly jet hypothesis proposed by Nagashima and co-authors was
579 motivated by their dust records derived off the Sea of Japan; *Nagashima et al.* [2011] showed
580 that East Asia is dustier during cold D/O phases. Some of the earliest studies of East Asian
581 dustiness are from Chinese Loess records, and the seminal *Porter and An* [1995] study showed
582 the link between North Atlantic cold events and dustiness. Most recently, a study by *An et al.*
583 [2012] of Qinghai lake sediments suggests that East Asia is dustier during Heinrich stadials
584 (including the Younger Dryas). They also show a gradual trend towards a less dusty climate
585 from the last glacial towards the present, suggesting a response to continental ice sheet changes
586 and/or CO₂.

587 East Asian dust changes have traditionally been interpreted as a proxy for changes to the
588 westerlies during the cold season. As argued by *Nagashima et al.* [2011], the key in linking
589 paleodust to jets and seasonality is in noting that East Asian dust is mostly a springtime
590 phenomenon. According to *Roe* [2009], dust outbreaks over Asia occur because of a particular
591 set of circumstances that occur uniquely in springtime, namely frequent cyclogenesis events over
592 the Mongolian Altai combined with strong cold air surges from Siberia. Combined, they
593 produce conditions suitable for dust entrainment into the atmosphere. *Nagashima et al.* [2011]
594 argued that the westerlies shifted southwards during cold D/O stages, which by the ‘Jet
595 Transition’ hypothesis would imply a delayed South-to-North jet transition and a longer Spring
596 (scenario B or C in **figure 5**).

597 More recently, *Nagashima et al.* [2013] have extended their hypothesis to the Holocene
598 climate, arguing that dust provenance – Gobi vs Taklimakan Desert – reflects changes to the
599 westerly jet path, with more dust from the latter relative to the former indicating an earlier

600 seasonal northward transition and longer summer. Applying this interpretation to the dust
601 provenance data indicates that in precessional phases with lower northern hemisphere summer
602 insolation, as well as during cold stadial events, the jet stays in a more southern position for a
603 greater part of the year (*Nagashima et al.*, 2007; *Nagashima et al.*, 2011). This is broadly
604 consistent with the jet hypothesis we present here. Neither the intensity nor upstream
605 interpretations readily explains changes to East Asian dustiness, though it should also be said
606 that neither is necessarily inconsistent.

607 7.2 *Spatially-varying evolution of East Asian rainfall during the Holocene*

608 Based on an analysis of a number of available proxy (non-speleothem) records across East Asia,
609 *An et al.* [2000] concluded that the ‘Holocene optimum’ climate occurred at different times
610 across different regions in China: generally, northwestern China rainfall peaked during the early
611 Holocene, central China during the mid-Holocene, and southeastern China during the late
612 Holocene (**figure 20a**).

613 This asynchronous peaking of the Holocene rainfall climate is not consistent if one treats
614 the East Asian summer monsoon as a contiguous whole, as is implied when paleoproxies are
615 interpreted as reflecting monsoon ‘intensification’. However, this observation can be made
616 consistent if one accounts for the various stages in East Asian rainfall seasonality. To illustrate,
617 we refer back to the CAM5 climate simulations introduced in section 4.1, where the 11,000 ybp
618 runs exhibited an earlier Meiyu onset and longer Summer rains as compared to the present-day
619 control. The annual mean rainfall difference between these two simulations is shown in **figure**
620 **20b**. The striking feature of this difference is the reduction to the rainfall over central China, in
621 contrast to the increase over northern China. This makes sense from a seasonality perspective,

622 since a longer Summer rainfall regime – supplying rainfall to northern China – also suggests a
623 shorter pre-Meiyu and Meiyu rainfall season that provides rainfall to central and southern China.

624 As the precessional influence works its way from the early Holocene to the late Holocene
625 and Northern Hemisphere summer insolation decreases, the hypothesis would predict a shorter
626 Summer rainfall regime and longer pre-Meiyu and Meiyu rainfall, bringing more rainfall to
627 central China. This would be qualitatively consistent with central China rainfall peaking in the
628 mid-Holocene.

629 **8. Discussion**

630 *8.1 Summary*

631 We advance a hypothesis for a central role played by the dynamics of East Asian rainfall
632 seasonality in East Asian paleoclimate changes, and in particular the changes to the seasonal
633 meridional position of the westerlies relative to the Tibetan Plateau. Today’s East Asian rainfall
634 seasonality exhibits quasi-stationary stages and abrupt transitions driven by the atmospheric
635 dynamics of the westerlies impinging on the Plateau, such that the meridional position of the
636 westerlies relative to Tibet defines the rainfall stage (See **figure 21** for a schematic). Given that
637 the meridional position of the westerlies is readily altered by paleoclimate forcings, the
638 suggestion is that East Asian seasonality also varies on longer timescales. Several studies have
639 previously proposed the role of seasonality (e.g. *Wang et al.*, 2001; *Cheng et al.* 2009b; *Clemens*
640 *et al.*, 2010), and Kana Nagashima and co-authors were the first to explicitly advance the role of
641 westerly jet changes as an explanation for their East Asian dust records (*Nagashima et al.*, 2011;
642 *Nagashima et al.*, 2013).

643 The *Jet Transition Hypothesis* as proposed here is that *changes to the seasonal meridional*
644 *position of the westerlies relative to the Tibetan Plateau drive rainfall climate changes over East*

645 *Asia on paleoclimate timescales.* Paleoclimate forcings – such as North Atlantic cooling, North
646 American ice sheets, global warmings and coolings, and orbital changes – are known to readily
647 change the position and strength of the westerlies.

648 Given that the spatial position of the Tibetan Plateau is fixed, the jet configuration during
649 each seasonal transition also remains the same, and so do the associated rainfall regimes (Spring,
650 pre-Meiyu, Meiyu or Summer). Thus, given how the westerlies change in past climate scenarios,
651 we can make qualitative predictions about when and how long each of the rainfall phases -
652 Spring, pre-Meiyu, Meiyu or Summer – occurred. Major changes arise if one or more phases do
653 not occur (e.g. Spring, pre-Meiyu and Meiyu occur, but not Summer). We then used objective
654 analysis modern-day observational data to show that interannual variations occur in the seasonal
655 transitions associated with the onset of the Meiyu, and again from the Meiyu to Summer; they
656 both involve the co-variation between the meridional position of the westerly jet and
657 precipitation. They serve to demonstrate that changes to the seasonal transitions and associated
658 westerly jet changes do, in fact, occur in reality.

659 To demonstrate the plausibility of the hypothesis and its predictions, we showed the results
660 of an atmospheric general circulation model (CAM5) for 11,000 years ago during a time of much
661 higher boreal summer insolation; in this scenario, the transition to Meiyu occurred earlier, and
662 Summer rains persisted longer, in line with earlier northward transition of the westerly jet. A
663 similar demonstration was made for a prototypical North Atlantic cold event, though the
664 modeled changes were smaller and less obvious than those for the precession example.

665 A concrete attempt was made to connect the hypothesis with $\delta^{18}\text{O}$ variations seen in
666 speleothem records, using the present-day seasonal cycle of $\delta^{18}\text{O}_p$ over East Asia as guide. The
667 key observation we exploited was that $\delta^{18}\text{O}_p$ was light during the summer over East Asia, which

668 we attributed to the low-level inflow of monsoonal moisture; since the westerly jet position
669 restricts the northward penetration of the monsoonal flow, variations in the former lead to spatial
670 variations in the $\delta^{18}\text{O}_p$. A thought experiment that kept East Asian climate in Spring conditions
671 (jet south of Plateau) during the summer months lead to a widespread increase in annual mean
672 $\delta^{18}\text{O}_p$ throughout East Asia (by around 2.5 per mil for Nanjing, less over southeastern China).
673 Given that the amplitude of D/O swings in the speleothem records was on the order of 2 per mil,
674 and precessional swings on the order of 3-4 per mil, it suggested that such conditions (Spring
675 throughout most of boreal summer) may have existed in the past climate.

676 The interpretation of a longer Spring during cold phases of North Atlantic D/O events is
677 consistent with the interpretation for increased dustiness and changes in the source area of dust,
678 as shown by *Nagashima et al.* [2011]. The observation of Holocene optimal rainfall shifting
679 from north China during the early Holocene, to central China during the mid Holocene, and
680 southeastern China during the late Holocene, also appears to be readily explainable by the
681 hypothesis. Lake records also indicate cold and dry conditions associated with stadial events,
682 which may be tied to dynamical changes in jet and a reduction in the northward penetration of
683 the monsoonal flow [*Liu et al.*, 2002; *Yi and Saito*, 2004; *Herzschuh*, 2006]. However, these data
684 are not necessarily inconsistent with other explanations of monsoonal change (i.e. arguments
685 about intensity or upstream changes in the monsoonal circulation).

686 8.2 *Lessons learned and the way forward*

687 We have demonstrated that seasonality is a viable hypothesis for interpreting East Asian
688 speleothem records. The unique strengths of this hypothesis are that

- 689 • We are relying on an analog that is already seen in the modern-day East Asian seasonal
690 cycle – as such, existence of the dynamics underlying this hypothesis is not in question.

691 There are also observed interannual variations in the timing of seasonal transitions linked
692 to westerly jet location, which further supports the control of jet position over
693 seasonality.

694 • It appears able to account for the spatial coherence of the speleothem $\delta^{18}\text{O}$ records over
695 East Asia, a distinct advantage over ‘intensity’ interpretations that do not readily explain
696 this coherence.

697 • It also appears to explain other paleoclimate indicators of climate changes, most notably
698 East Asian dust records and the spatial progression of optimal rainfall conditions during
699 the Holocene. As such, it holds an advantage over the ‘intensity’ and ‘upstream’
700 hypotheses that do not address these observations.

701 • The hypothesis is testable. By determining the impact of jet transition timing on present
702 day climate, we obtain a detailed spatial signature of the expected climate impacts under
703 modified seasonality, allowing for a detailed comparison to paleoproxy records at
704 specific locations. Using observed patterns rather than modeling results is a distinct
705 advantage, as relatively few climate models simulate the seasonal transitions of the East
706 Asian monsoon with fidelity, and even if they do there are spatial biases to the simulated
707 climate and changes.

708 We end off with a discussion of how this hypothesis can be moved forward. A detailed
709 comparison with a complete set of paleoproxy records could be done, alongside the spatial
710 predictions of climate changes that can be inferred from observational analogs; these would
711 include various lake and pollen records, dust records, speleothems, and tree ring records. While
712 we have some idea of how the changes should look for large paleoclimate events such as the
713 Younger Dryas and early-mid Holocene, we do not yet have a good sense of how ‘smaller’

714 climate changes such as those occurring over the last millennia should look like. Such a
715 comparison could extend this hypothesis towards the more recent paleoclimate.

716 We have argued that the hypothesis can plausibly explain the speleothem $\delta^{18}\text{O}$ variations
717 including the spatial coherence; but a quantitative test of this hypothesis is clearly needed with a
718 modeling study. However, such a model also needs to be able to correctly simulate the quasi-
719 stationary stages of East Asian rainfall. Our experience suggests that relatively few models do
720 this correctly, and that furthermore sufficient horizontal resolution is necessary to simulate its
721 relatively fine-scale features. The CAM5 model at 1° resolution that we used for our paleo
722 simulations is such a model, but as of writing, water isotopes for that model have yet to be
723 implemented.

724 Targeted paleoproxy observations are important for moving the hypothesis forward. A
725 potentially exciting development is the recent result by *Orland et al. (2014)* where they sampled
726 Chinese stalagmites at sub-annual resolution to reveal seasonal variations in $\delta^{18}\text{O}$ and how that
727 varied over the last glacial and Holocene. They infer that the proportion of summer monsoon
728 rainfall was larger during the Holocene and Bølling-Allerød than during the Younger Dryas, in
729 apparent support of the hypothesis. In general, their result points to the central role of
730 seasonality in explaining East Asian paleomonsoon changes.

731 A stronger dynamical basis is needed to tie the character of the westerlies to the
732 seasonality of East Asian monsoon rainfall. The meridional position of the westerly jet relative
733 to the Tibetan Plateau appears to be a dominant control, but the structure of the westerlies is 3-
734 dimensional so this criterion is likely too simplistic. Do other properties of the westerlies
735 matter? Three other features come to mind: first, the strength of the westerlies – the transition
736 from Meiyu to Summer rainfall is marked not just by northward shift but also by a weakening,

737 signaling a weakening of the Meiyu front. Second, the vertical structure of the westerlies, in
738 particular distinguishing the barotropic to baroclinic components of the jet structure – the
739 barotropic component is by nature more affected by physical presence of the Tibetan Plateau.
740 Third, the width of the westerly belt: *Son et al.* [2009] found in an idealized general circulation
741 model study that the effect of topography on downstream storm-track intensity differed
742 significantly on whether the background flow was a weak double jet or a strong single jet.

743 Furthermore, other factors could affect the seasonal transitions of East Asian rainfall. For
744 example, *Hsu and Lin* [2007] found that the interannual ‘tripole pattern’ of summer East Asian
745 rainfall anomalies – which we associated with the variability in the Meiyu to Summer transition
746 (section 3) – is closely associated with two wavelike patterns, namely the Pacific-Japan pattern
747 and Silk Road pattern. Both patterns are associated with Rossby wave forcing impinging on the
748 East Asian circulation, and involve a significant meridional flow component; thus, stationary
749 wave patterns could likely factor in controlling the Meiyu to Summer transition. Finally, factors
750 that are traditionally considered in the variability of the East Asian monsoon, namely the
751 magnitude of land-ocean temperature contrasts, heating over the Tibetan Plateau, and the
752 strength of the Western North Pacific subtropical high and changes to the Western North Pacific
753 summer monsoon must be considered. The challenge is to incorporate the role of the westerlies
754 within the ‘traditional’ interpretive framework to derive a more complete theory for the East
755 Asian paleomonsoon.

756 **9. Acknowledgements**

757 This work started from a graduate seminar on the East Asian paleomonsoon taught at UC
758 Berkeley by JC and IF in the Spring of 2013. We acknowledge support from NSF grants AGS-
759 1405479 (to JC) and EAR-0909195 (to IF); JC also acknowledges support from a Visiting

760 Associate Professorship at Academia Sinica during Spring 2014, funded by the Consortium for
761 Climate Change Study under the auspices of the Ministry of Science and Technology (MOST),
762 Taiwan. CHW was also supported by MOST under grant 100-2119-M-001-029-MY5. Reinhard
763 Schiemann kindly provided the jet occurrence data used in figure 7. We thank Zhisheng An,
764 David Battisti, Huang-Hsiung Hsu, Shang-Ping Xie, Wenwen Kong and Kristina Løfman for
765 valuable discussions. JC thanks the proprietors and staff of Fortunate Coffee for their hospitality
766 during the writing of the manuscript.

767

768 **10. References**

- 769 Academia Sinica Staff Members (1957), On the General Circulation of Eastern Asia (I). *Tellus*
770 *A*, **9(4)**, 432 - 446
- 771 Academia Sinica Staff Members (1958a), On the General Circulation of Eastern Asia (II). *Tellus*
772 *A*, **10(1)**, 58 - 75
- 773 Academia Sinica Staff Members (1958b), On the General Circulation of Eastern Asia (III).
774 *Tellus A*, **10(3)**, 299-312
- 775 An, Z., S. C. Porter, J. E. Kutzbach, W. Xihao, W. Suming, L. Xiaodong, L. Xiaoqiang, and Z.
776 Weijian (2000), Asynchronous Holocene optimum of the East Asian monsoon, *Quaternary*
777 *Science Reviews*, *19(8)*, 743-762, doi:[http://dx.doi.org/10.1016/S0277-3791\(99\)00031-1](http://dx.doi.org/10.1016/S0277-3791(99)00031-1).
- 778 An, Z. S., et al. (2012), Interplay between the Westerlies and Asian monsoon recorded in Lake
779 Qinghai sediments since 32 ka, *Sci Rep-Uk*, *2*, doi:Artn 619
780 Doi 10.1038/Srep00619.
- 781 Berger A. (1978). Long-term variations of daily insolation and Quaternary climatic changes.
782 *Journal of Atmospheric Science*, *35(12)*, 2362-2367.
- 783 Bretherton, C. S., C. Smith, and J. M. Wallace (1992), An intercomparison of methods for
784 finding coupled patterns in climate data, *Journal of Climate*, *5(6)*, 541-560.
- 785 Chang, C., Y. Zhang, and T. Li (2000), Interannual and interdecadal variations of the East Asian
786 summer monsoon and tropical Pacific SSTs. Part I: Roles of the subtropical ridge, *Journal of*
787 *Climate*, *13(24)*, 4310-4325.
- 788 Chen, J., and S. Bordoni (2014), Orographic Effects of the Tibetan Plateau on the East Asian
789 Summer Monsoon: An energetic perspective, *Journal of Climate*(2014).

790 Cheng, H., et al. (2009a), Timing and structure of the 8.2 kyr B.P. event inferred from $\delta^{18}\text{O}$
791 records of stalagmites from China, Oman, and Brazil, *Geology*, 37(11), 1007-1010,
792 doi:10.1130/g30126a.1.

793 Cheng, H., Edwards, R. L., Broecker, W. S., Denton, G. H., Kong, X., Wang, Y., Zhang, R., and
794 Wang, X. (2009b). Ice age terminations. *Science*, 326(5950), 248-252.

795 Clemens, S. C., W. L. Prell, and Y. Sun (2010), Orbital-scale timing and mechanisms driving
796 Late Pleistocene Indo-Asian summer monsoons: Reinterpreting cave speleothem $\delta^{18}\text{O}$,
797 *Paleoceanography*, 25(4).

798 Cvijanovic, I., and J. C. Chiang (2013), Global energy budget changes to high latitude North
799 Atlantic cooling and the tropical ITCZ response, *Climate dynamics*, 40(5-6), 1435-1452.

800 Dansgaard, W. (1964), Stable isotopes in precipitation, *Tellus*, 16(4), 436-468.

801 Dayem, K. E., P. Molnar, D. S. Battisti, and G. H. Roe (2010), Lessons learned from oxygen
802 isotopes in modern precipitation applied to interpretation of speleothem records of
803 paleoclimate from eastern Asia, *Earth and Planetary Science Letters*, 295(1), 219-230.

804 Ding, Y., and J. C. L. Chan (2005), The East Asian summer monsoon: an overview, *Meteorology
805 and Atmospheric Physics*, 89(1-4), 117-142, doi:10.1007/s00703-005-0125-z.

806 Herzsich, U. (2006), Paleo-moisture evolution in monsoonal Central Asia during the last
807 50,000 years. *Quaternary Science Reviews* 25: 163 - 178

808 Holton JR. 2004. An Introduction to Dynamic Meteorology. Boston, MA: Elsevier. 529 pp. 4th
809 ed.

810 Hsu, H.-H., and S.-M. Lin (2007), Asymmetry of the tripole rainfall pattern during the East
811 Asian summer, *Journal of Climate*, 20(17), 4443-4458.

812 Hsu, H. H., and X. Liu (2003), Relationship between the Tibetan Plateau heating and East Asian
813 summer monsoon rainfall, *Geophysical Research Letters*, 30(20).

814 Hu, Z.-Z., S. Yang, and R. Wu (2003), Long-term climate variations in China and global
815 warming signals, *Journal of Geophysical Research*, 108(D19), 4614.

816 Huffman, G. J., R. F. Adler, D. T. Bolvin, G. Gu, E. J. Nelkin, K. P. Bowman, Y. Hong, E. F.
817 Stocker, D. B. Wolff, 2007: The TRMM multi-satellite precipitation analysis: Quasi-global,
818 multi-year, combined-sensor precipitation estimates at fine scale. *J. Hydrometeor.*, 8(1), 38-55.

819 Huybers, P., and I. Eisenman, 2006. Integrated summer insolation calculations. NOAA/NCDC
820 Paleoclimatology Program Data Contribution #2006-079.

821 Johnson, K. R., and B. L. Ingram (2004), Spatial and temporal variability in the stable isotope
822 systematics of modern precipitation in China: implications for paleoclimate reconstructions,
823 *Earth and Planetary Science Letters*, 220(3), 365-377.

824 Kalnay, E., et al. (1996), The NCEP/NCAR 40-Year Reanalysis Project, *Bulletin of the*
825 *American Meteorological Society*, 77(3), 437-471.

826 Kanamitsu, M., W. Ebisuzaki, J. Woollen, S.-K. Yang, J. Hnilo, M. Fiorino, and G. Potter
827 (2002), NCEP–DOE AMIP-II Reanalysis (R-2), *Bulletin of the American Meteorological*
828 *Society*, 83(11).

829 Kosaka, Y., & Nakamura, H. (2010). Mechanisms of meridional teleconnection observed
830 between a summer monsoon system and a subtropical anticyclone. Part I: The Pacific-
831 Japan pattern. *Journal of Climate*, 23(19), 5085-5108.

832 Kosaka, Y., Xie, S. P., & Nakamura, H. (2011). Dynamics of Interannual Variability in Summer
833 Precipitation over East Asia*. *Journal of Climate*, 24(20), 5435-5453.

834 Kummerow, C., W. Barnes, T. Kozu, J. Shiue, and J. Simpson (1998), The Tropical Rainfall
835 Measuring Mission (TRMM) sensor package. *J. Atmos. Oceanic Technol.*, **15**, 809–817.

836 Kutzbach, J. E. (1981), Monsoon Climate of the Early Holocene - Climate Experiment with the
837 Earths Orbital Parameters for 9000 Years Ago, *Science*, *214*(4516), 59-61.

838 Lee, J.-E., and I. Fung (2008), “Amount effect” of water isotopes and quantitative analysis of
839 post-condensation processes, *Hydrol. Process.*, *22*(1), 1-8, doi:10.1002/hyp.6637.

840 Lee, J.-E., C. Risi, I. Fung, J. Worden, R. A. Scheepmaker, B. Lintner, and C. Frankenberg
841 (2012), Asian monsoon hydrometeorology from TES and SCIAMACHY water vapor isotope
842 measurements and LMDZ simulations: Implications for speleothem climate record
843 interpretation, *Journal of Geophysical Research: Atmospheres*, *117*(D15), D15112,
844 doi:10.1029/2011jd017133.

845 Liang, X.-Z., and W.-C. Wang (1998), Associations between China monsoon rainfall and
846 tropospheric jets, *Quarterly Journal of the Royal Meteorological Society*, *124*(552), 2597-
847 2623, doi:10.1002/qj.49712455204.

848 Lin, Z., & Lu, R. (2008). Abrupt northward jump of the East Asian upper-tropospheric jet
849 stream in mid-summer. *Journal of the Meteorological Society of Japan*, **86**(6), 857-866.

850 Liu, X., J. Shen, S. Wang, X. Yang, G. Tong, E. Zhang. 2002. A 16000 year pollen record of
851 Qinghai Lake and its paleoclimate and paleoenvironment. *Chinese Science Bulletin* *47*(22):
852 1931 - 1936.

853 Liu, Y. H., G. M. Henderson, C. Y. Hu, A. J. Mason, N. Charnley, K. R. Johnson, and S. C. Xie
854 (2013), Links between the East Asian monsoon and North Atlantic climate during the 8,200
855 year event, *Nature Geosci*, *6*(2), 117-120,

856 doi:<http://www.nature.com/ngeo/journal/v6/n2/abs/ngeo1708.html> - supplementary-
857 information.

858 Liu, Y., J. C. H. Chiang, C. Chou, and C. M. Patricola (2014), Atmospheric Teleconnection
859 Mechanisms of extratropical North Atlantic SST influence on Sahel Rainfall. *Climate*
860 *Dynamics*, **43**, 2797-2811. DOI:10.1007/s00382-014-2094-8,

861 Liu, Z., et al. (2014), Chinese cave records and the East Asia Summer Monsoon, *Quaternary*
862 *Science Reviews*, 83(0), 115-128, doi:<http://dx.doi.org/10.1016/j.quascirev.2013.10.021>.

863 Lu, R., & Lin, Z. (2009). Role of subtropical precipitation anomalies in maintaining the
864 summertime meridional teleconnection over the western North Pacific and East Asia. *Journal*
865 *of Climate*, 22(8), 2058-2072.

866 Molnar, P., W. R. Boos, and D. S. Battisti (2010), Orographic Controls on Climate and
867 Paleoclimate of Asia: Thermal and Mechanical Roles for the Tibetan Plateau, *Annu Rev Earth*
868 *Pl Sc*, 38, 77-102, doi:Doi 10.1146/Annurev-Earth-040809-152456.

869 Nagashima, K., R. Tada, H. Matsui, T. Irino, A. Tani, and S. Toyoda (2007), Orbital-and
870 millennial-scale variations in Asian dust transport path to the Japan Sea, *Palaeogeography,*
871 *Palaeoclimatology, Palaeoecology*, 247(1), 144-161.

872 Nagashima, K., R. Tada, A. Tani, Y. Sun, Y. Isozaki, S. Toyoda, and H. Hasegawa (2011),
873 Millennial-scale oscillations of the westerly jet path during the last glacial period, *Journal of*
874 *Asian Earth Sciences*, 40(6), 1214-1220, doi:<http://dx.doi.org/10.1016/j.jseaes.2010.08.010>.

875 Nagashima, K., and R. Tada (2012): Teleconnection mechanism between millennial-scale Asian
876 Monsoon dynamics and North Atlantic climate. *PAGES news*, **20**, 2, 64-65.

877 Nagashima, K., R. Tada, and S. Toyoda (2013), Westerly jet-East Asian summer monsoon
878 connection during the Holocene, *Geochemistry, Geophysics, Geosystems*, 14(12), 5041-5053.

879 Neale, R. B., C. Chen, A. Gettelman, P. Lauritzen, S. Park, D. Williamson, A. Conley, R. Garcia,
880 D. Kinnison, and J. Lamarque (2010), Description of the NCAR community atmosphere model
881 (CAM 5.0), *NCAR Tech. Note NCAR/TN-486+ STR*.

882 Orland, I., Edwards, R. L. , Cheng, H., Kozdon, R., and Valley, J. (2014), **Seasonal-Resolution**
883 **δ 18O in Speleothems by Ion Microprobe: Revealing Asian Monsoon Dynamics**, Abstract
884 **PP31B-1132** presented at 2014 Fall Meeting, AGU, San Francisco, Calif., 15-19 Dec.

885 Park, H. S., J. C. H. Chiang, and S. Bordoni (2012), The Mechanical Impact of the Tibetan
886 Plateau on the Seasonal Evolution of the South Asian Monsoon, *Journal of Climate*, 25(7),
887 2394-2407, doi:10.1175/jcli-d-11-00281.1.

888 Pausata, F. S. R., D. S. Battisti, K. H. Nisancioglu, and C. M. Bitz (2011), Chinese stalagmite
889 delta O-18 controlled by changes in the Indian monsoon during a simulated Heinrich event,
890 *Nature Geoscience*, 4(7), 474-480, doi:Doi 10.1038/Ngeo1169.

891 Porter, S., and A. Zhisheng (1995), Correlation Between Climate Events in the North Atlantic
892 and China During the Last Glaciation, *Nature*, 375, 305-308.

893 Roe, G. (2009), On the interpretation of Chinese loess as a paleoclimate indicator, *Quaternary*
894 *Research*, 71(2), 150-161, doi:http://dx.doi.org/10.1016/j.yqres.2008.09.004.

895 Saha, S., and Coauthors (2010), The NCEP Climate Forecast System Reanalysis. *Bull. Amer.*
896 *Meteor. Soc.*, **91(8)**, 1015–1057.

897 Sampe, T., and S.-P. Xie (2010), Large-Scale Dynamics of the Meiyu-Baiu Rainband:
898 Environmental Forcing by the Westerly Jet*, *Journal of Climate*, 23(1), 113-134,
899 doi:10.1175/2009jcli3128.1.

900 Schiemann, R., D. Lüthi, and C. Schär (2009), Seasonality and Interannual Variability of the
901 Westerly Jet in the Tibetan Plateau Region*, *Journal of Climate*, 22(11), 2940-2957,
902 doi:10.1175/2008jcli2625.1.

903 Schneider, U., T. Fuchs, A. Meyer-Christoffer and B. Rudolf (2008): Global Precipitation
904 Analysis Products of the GPCC. Global Precipitation Climatology Centre (GPCC), DWD,
905 Internet Publikation, 1-12.

906 Son, S. W., M. F. Ting, and L. M. Polvani (2009), The Effect of Topography on Storm-Track
907 Intensity in a Relatively Simple General Circulation Model, *Journal of the Atmospheric*
908 *Sciences*, 66(2), 393-411, doi:10.1175/2008jas2742.1.

909 Ueda, H., Ohba, M., & Xie, S. P. (2009). Important Factors for the Development of the Asian-
910 Northwest Pacific Summer Monsoon. *Journal of Climate*, 22(3), 649-669.

911 Uppala, S. M., et al. (2005), The ERA-40 re-analysis, *Quarterly Journal of the Royal*
912 *Meteorological Society*, 131(612), 2961-3012, doi:10.1256/qj.04.176.

913 Wang, Y. J., H. Cheng, R. L. Edwards, Z. S. An, J. Y. Wu, C. C. Shen, and J. A. Dorale (2001),
914 A high-resolution absolute-dated Late Pleistocene monsoon record from Hulu Cave, China,
915 *Science*, 294(5550), 2345-2348.

916 Wang, Y. J., H. Cheng, R. L. Edwards, X. G. Kong, X. H. Shao, S. T. Chen, J. Y. Wu, X. Y.
917 Jiang, X. F. Wang, and Z. S. An (2008), Millennial- and orbital-scale changes in the East Asian
918 monsoon over the past 224,000 years, *Nature*, 451(7182), 1090-1093, doi:Doi
919 10.1038/Nature06692.

920 Weng, H., K.-M. Lau, and Y. XUE (1999), Multi-scale summer rainfall variability over China
921 and its long-term link to global sea surface temperature variability, *Journal of the*
922 *Meteorological Society of Japan*, 77(4), 845-857.

923 Wu, G., Y. Liu, Q. Zhang, A. Duan, T. Wang, R. Wan, X. Liu, W. Li, Z. Wang, and X. Liang
924 (2007), The Influence of Mechanical and Thermal Forcing by the Tibetan Plateau on Asian
925 Climate, *J. Hydrometeorol.*, 8(4), 770-789, doi:10.1175/jhm609.1.

926 Wu, Z. H., and N. E. Huang (2004), A study of the characteristics of white noise using the
927 empirical mode decomposition method, *Proceedings of the Royal Society of London Series a-
928 Mathematical Physical and Engineering Sciences*, 460(2046), 1597-1611.

929 Xu, Q. (2001), Abrupt change of the mid-summer climate in central east China by the influence
930 of atmospheric pollution, *Atmos. Environ.*, 35(30), 5029-5040.

931 Yeh, T.-C., S. Tao, and M. Li (1959), The abrupt change of circulation over the Northern
932 Hemisphere during June and October, *The Atmosphere and the Sea in Motion*, 249-267.

933 Yi, S., and Y. Saito. 2004. Latest Pleistocene climate variation of the East Asian monsoon from
934 pollen records of two East China regions. *Quaternary International* 121(1): 75 - 87.

935 Yu, R., B. Wang, and T. Zhou (2004), Tropospheric cooling and summer monsoon weakening
936 trend over East Asia, *Geophysical Research Letters*, 31(22).

937 Yuan, D., H. Cheng, R. L. Edwards, C. A. Dykoski, M. J. Kelly, M. Zhang, J. Qing, Y. Lin, Y.
938 Wang, and J. Wu (2004), Timing, duration, and transitions of the last interglacial Asian
939 monsoon, *Science*, 304(5670), 575-578.

940 Zhou, T., D. Gong, J. Li, and B. Li (2009), Detecting and understanding the multi-decadal
941 variability of the East Asian summer monsoon recent progress and state of affairs,
942 *Meteorologische Zeitschrift*, 18(4), 455-467.

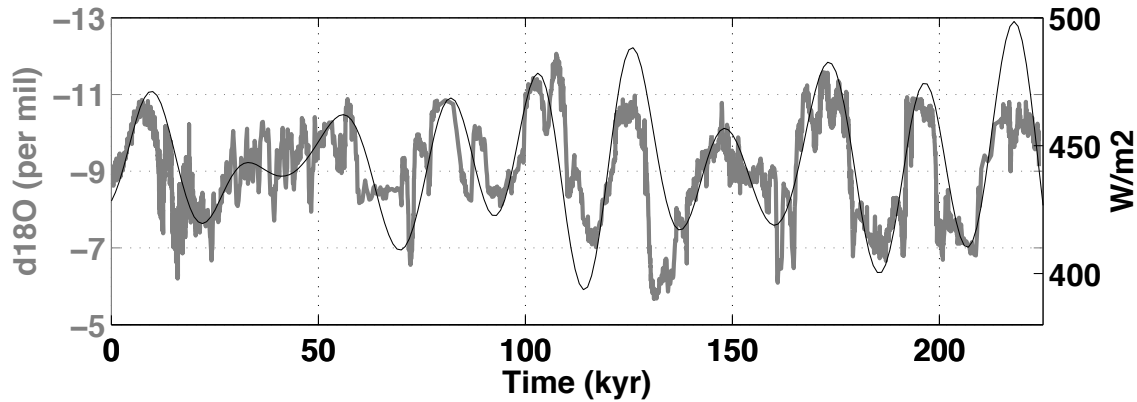


Figure 1. Thick gray line (left scale) is speleothem $\delta^{18}O$ record from Wang et al. (2008), and thin black line is July 21 insolation (right scale). The speleothem $\delta^{18}O$ record is interpreted as variation in the East Asian rainfall climate over the last 220,000 years. The record is stitched from several speleothems from the Hulu, Dongge and Sanbao cave sites in China. They clearly show changes on precessional timescales (as compared to the insolation line). They also fluctuate in sync with D/O events during the last glacial period. The Wang et al. [2008] speleothem data was obtained from the NOAA National Climatic Data Center (<http://www.ncdc.noaa.gov>). The insolation curve was computed from a MATLAB code by Huybers and Eisenman [2006], following the algorithm by Berger [1978].

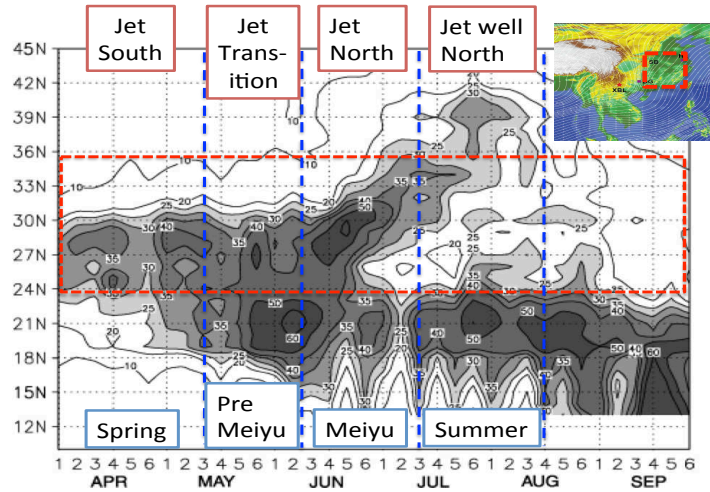


Figure 2. Latitude-time section of 5-day mean rainfall over eastern China (110-120E, see inset) from April to September averaged for 1961-1990. Units of rainfall are mm, and regions of heavy rainfall (>25mm) are shaded. Also marked (blue dashed lines) are the stages in the rainfall and relationship to jet position. The red dashed line corresponds to latitudes shown in the map inset. Figure originally from Ding and Chan [2005], figure 7; identification of the rainfall stages, and map inset, are added by the authors.

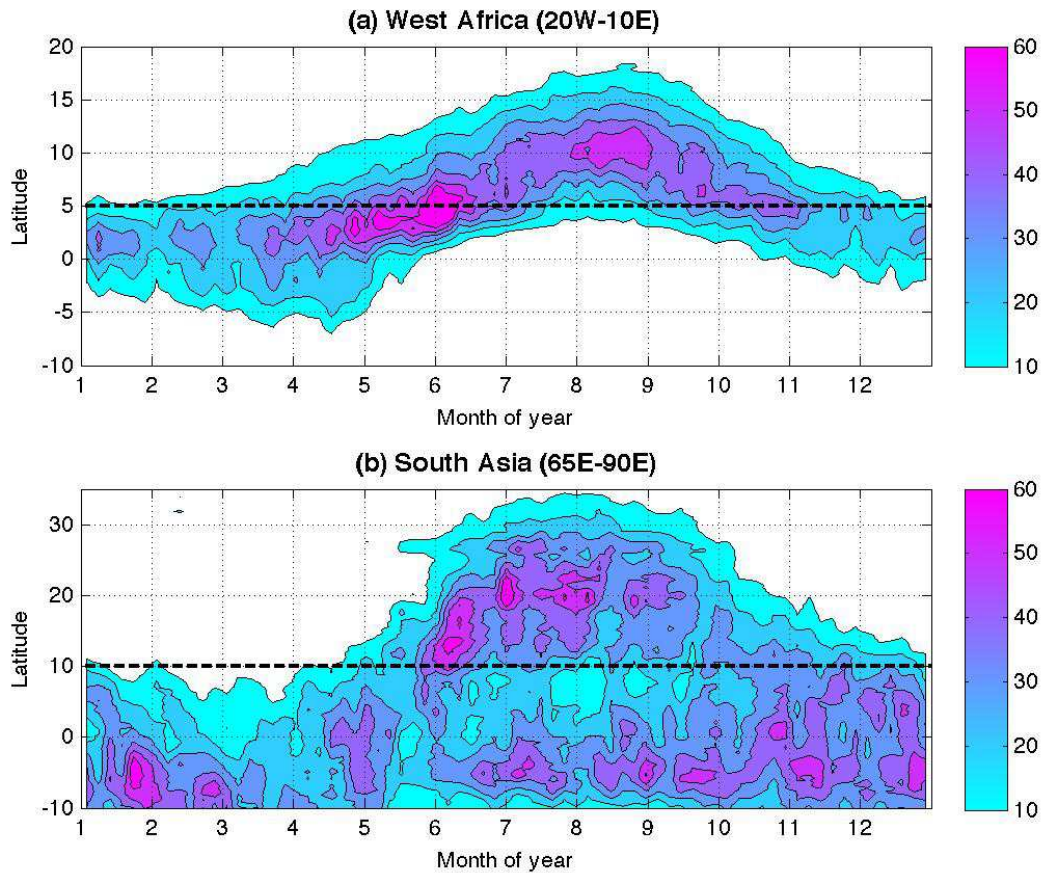


Figure 3. Latitude-Time plots of 5-day mean rainfall for two northern hemisphere monsoon systems. **(a)** West Africa (20°W-10°E); and **(b)** South Asia (65°E-90°E). Data is from the Tropical Rainfall Measuring Mission (TRMM) 3B42 v7 daily rainfall from 1 Jan 1998 to 31 Dec 2013 [Huffman et al., 2007]. Units are mm, and the x-axis is the month of the year. Dashed line indicates the approximate latitude location of the land-ocean boundary for the regions.

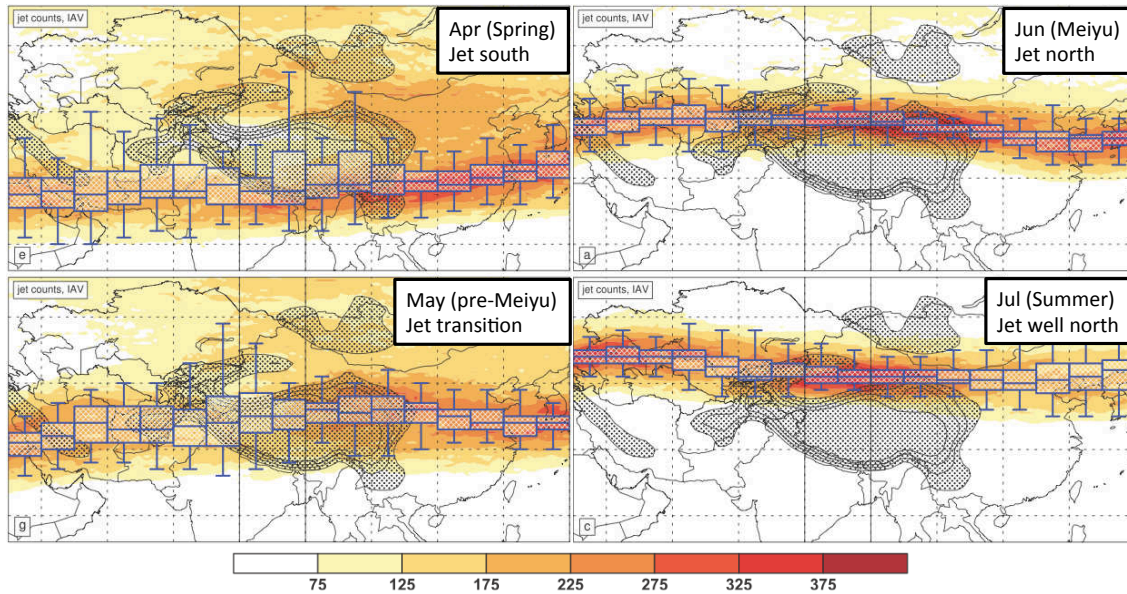


Figure 4. Seasonal transition of the westerly jet from south to north of the Plateau, and their association with the rainfall regimes over East Asia. Total jet occurrence counts (shaded) and interannual variability of jet latitude (boxes) for April to July as computed by Schiemann et al. [2009] from 6-hourly ERA-40. A ‘jet occurrence’ is defined at a location if wind speed is a local maximum somewhere in the vertical column, that it exceeds 30m/s, and is westerly. Associated with each jet position is the particular rainfall regime, indicated by the text. Original figure is taken from Schiemann et al. [2009], and modified by the authors; in particular, the identification of the rainfall stages is added by the authors.

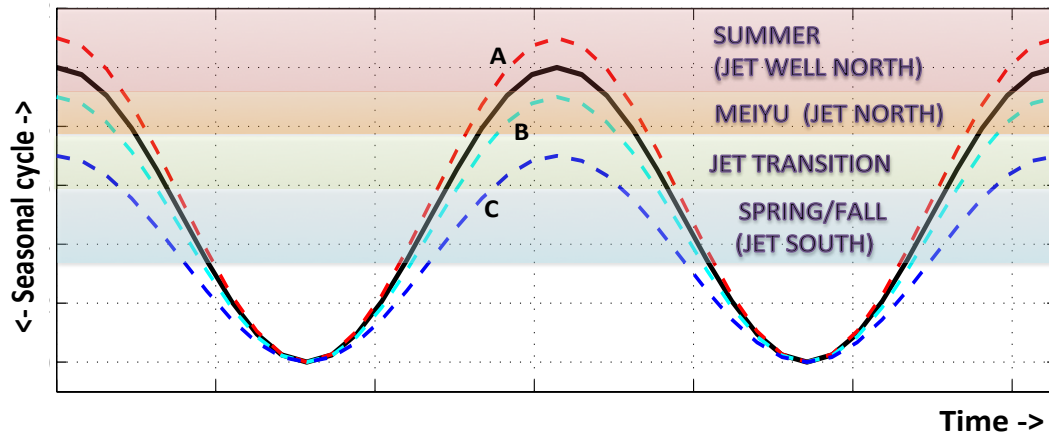


Figure 5. Schematic of an idealized East Asian seasonal cycle relative to rainfall/jet transitions. The 'normal' seasonal cycle is given in the solid black line. Idealized scenarios (dashed lines) illustrate how a delay in the south to north jet transition leads to changes in the East Asian rainfall climate. Scenario 'A' (red) is for an earlier jet transition, whereas 'B' (cyan) occurs later. In scenario 'C' (blue), the jet does not make the full transition to the North of the Plateau.

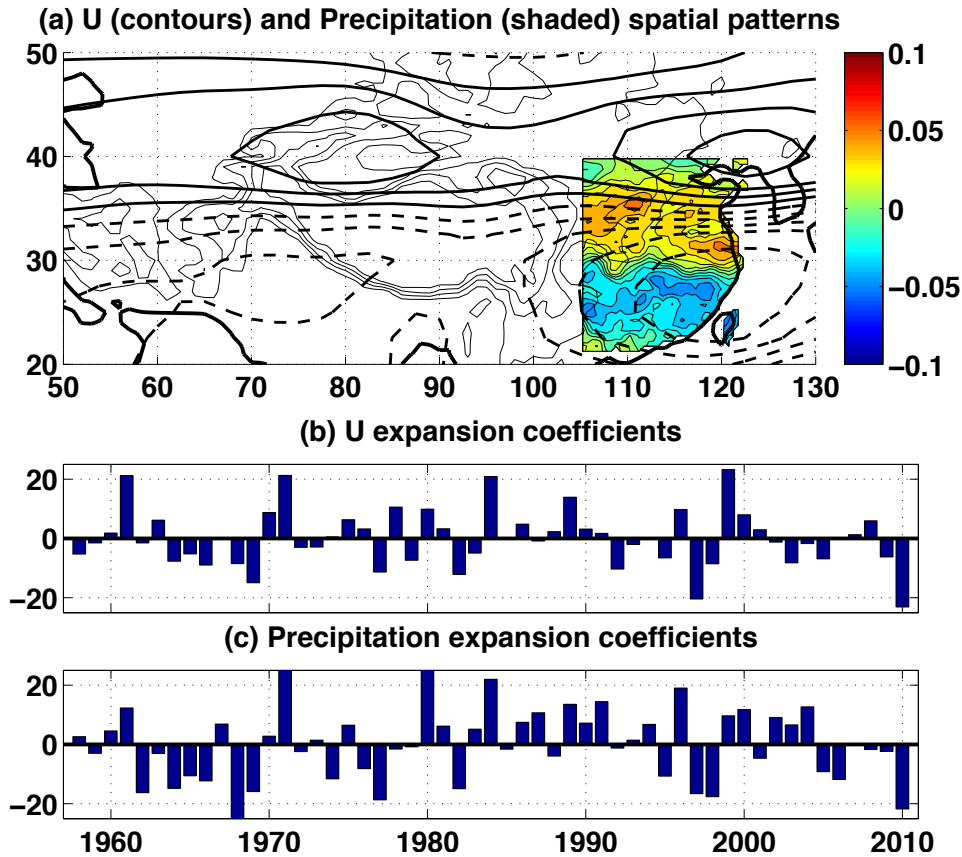


Figure 6. First mode of an MCA analysis 1958-2010 on normalized June monthly mean upper tropospheric zonal winds (left field) and June normalized East Asian rainfall (right field). See text for details. The first mode explains 56% of the combined variance. **(a)** Spatial pattern of the zonal wind (left) field (contours, dashed are negative values) and of precipitation (right) field (shaded); **(b)** zonal wind expansion coefficients; and **(c)** precipitation expansion coefficients. Mode 1 captures the coupled interannual variation in zonal wind over Asia and precipitation over East Asia, with a more northern jet associated with more rains in the north and less in the south. We interpret this pattern to be an earlier onset of the Meiyu with a more northward jet.

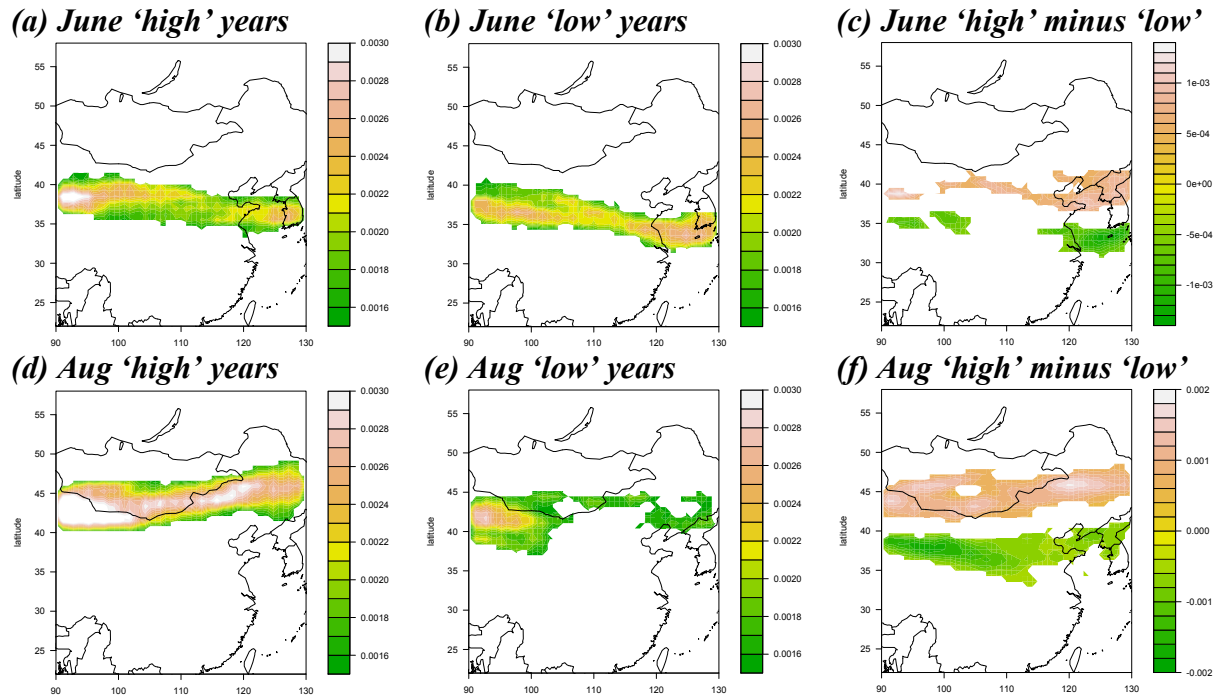


Figure 7. Composite of jet occurrences contrasting ‘high’ and ‘low’ years in the U expansion coefficients of figure 6. We use the jet occurrence data as computed by Schiemann et al. [2009], and add up all the jet counts from June 11-20 for specified years between 1958 and 2001. The plots shown are normalized kernel-density estimates for the jet counts composited in this way. ‘High’ (‘low’) years are defined to be years when the U expansion coefficient is larger (smaller) than $+0.1$ (-0.1). **(a)** Composite for ‘high’ years; **(b)** composite for ‘low’ years; and **(c)** ‘high’ minus ‘low’. **(d) through (f)** are the same as for **(a)** through **(c)**, but for August 1-10 and using the U -expansion coefficients of the July-August MCA1 in Figure 10. For the ‘high’ and ‘low’ plots, we only show values exceeding 1.5×10^{-3} , and for the ‘high minus low’ we only show values whose magnitude exceed 0.5×10^{-3} .

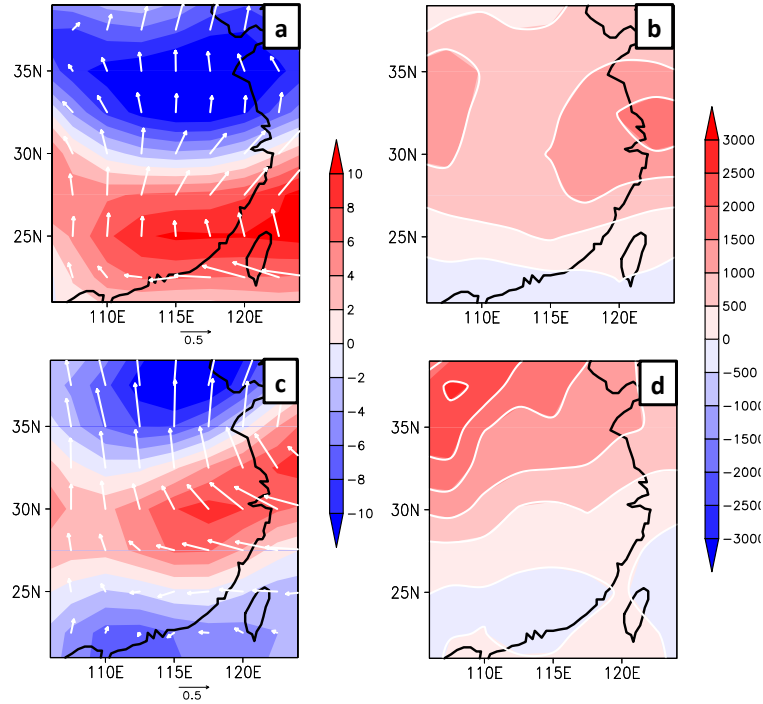


Figure 8. Regression of the normalized MCA mode 1 U expansion coefficients on **(a)** NCEP June 925mb winds (reference vector is 0.5 m/s) and 500mb pressure vertical velocity (shaded; units are $\times 10^{-3} \text{Pa/s}$, contour interval is $2 \times 10^{-3} \text{Pa/s}$), with negative values implying anomalous ascent; **(b)** NCEP June moist static energy at 925mb (units are J/kg, contour interval is 500 J/kg). **(c) and (d):** same as (a) and (b), but for Jul-Aug fields.

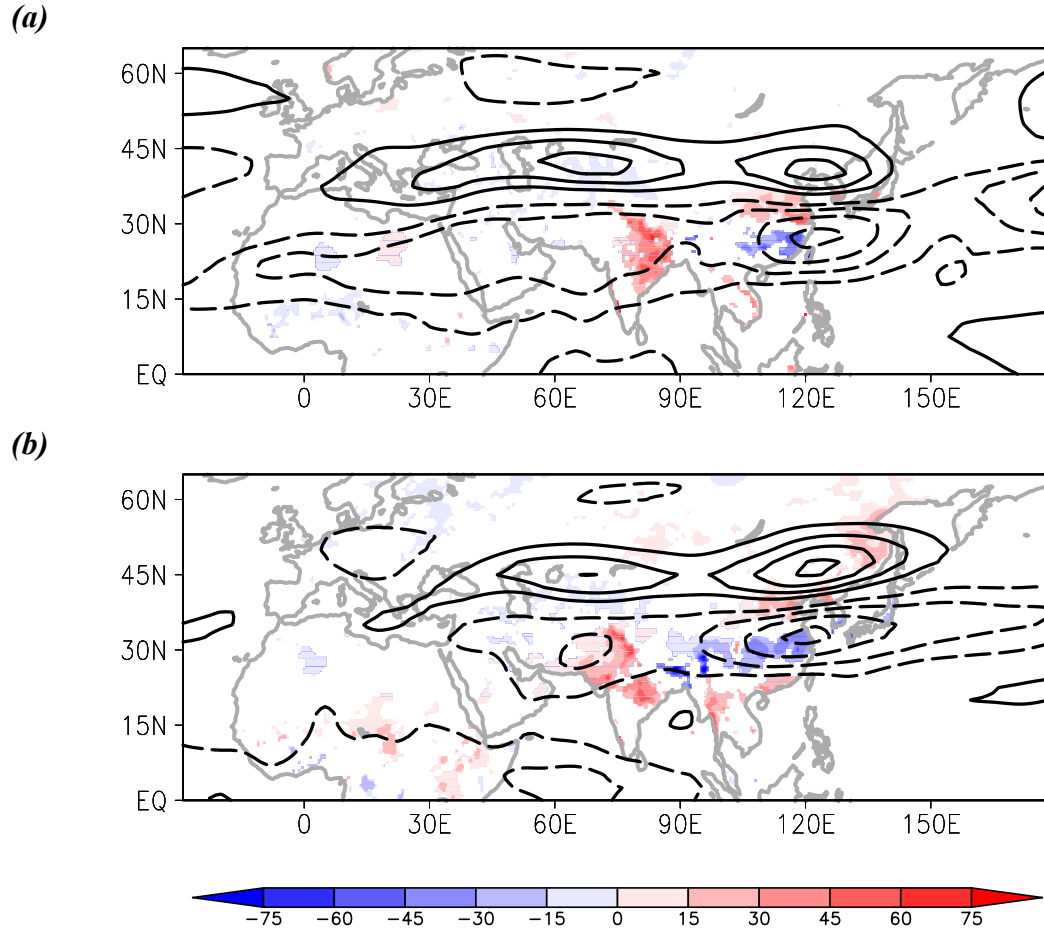


Figure 9. (a) Regression of the June MCA mode 1 normalized U expansion coefficients 1958-2010 on June precipitation (shaded; units are mm/month per standard deviation of index) and June 100-500mb averaged zonal wind (contour interval 1m/s per unit standard deviation, dashed lines are negative; zero contour not shown) over Asia. For precipitation, values are only plotted if the corresponding correlation magnitude exceeds 0.229 (90% significance level). (b) Same as (a), but for the Jul-Aug MCA mode 1 U expansion coefficients on Jul-Aug precipitation and July-Aug 100-500mb averaged zonal wind. In both (a) and (b), the analysis reveals a northward shift in the westerly jet axis across Central and East Asia associated with an earlier transition of the rainfall regime. For the June case (a), the effects of an earlier northward jet transition is evident in the spatial pattern of the precipitation over China – less rainfall over to the south of $\sim 30^\circ\text{N}$, and more to the north. For the July-Aug case (b), a tripole pattern is seen over China with more rainfall over northern and southern China, and less over central China. Intriguingly, in both the June and July-Aug cases, there is also a significant increase in rainfall over the northern India.

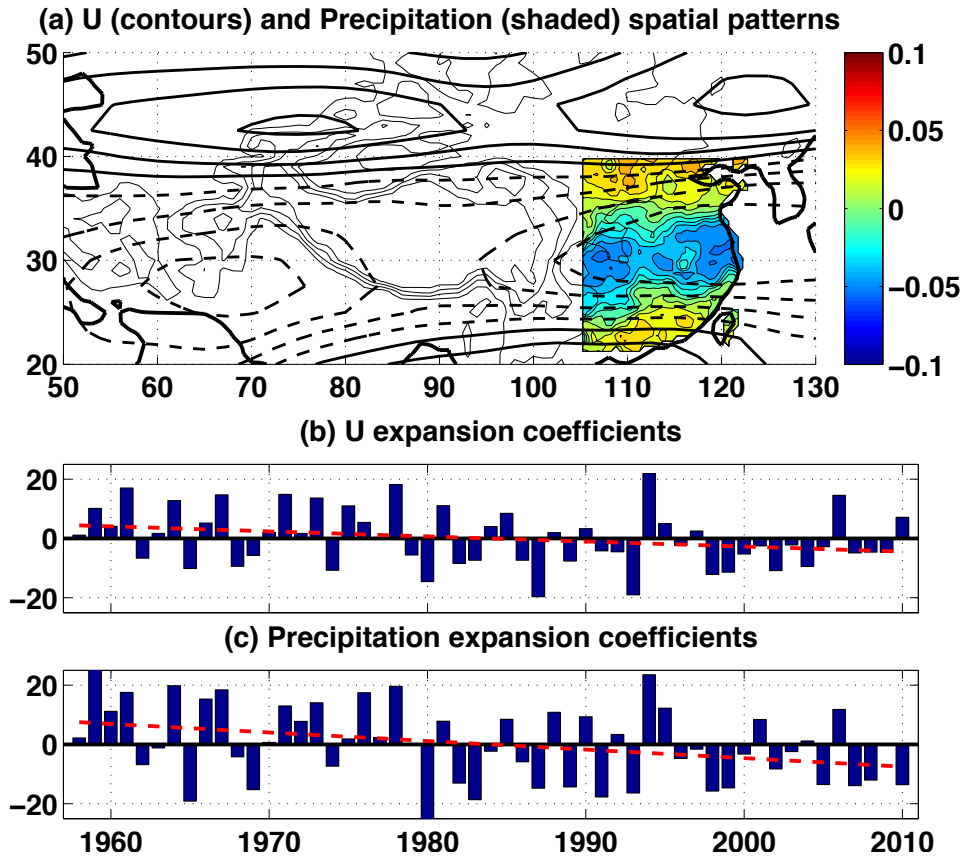


Figure 10. First mode of an MCA analysis 1958-2010 on normalized Jul-Aug monthly mean upper tropospheric zonal winds (left field) and Jul-Aug normalized East Asian rainfall (right field). See text for details. The first mode explains 56% of the combined variance. **(a)** Spatial pattern of the zonal wind (contours; dashed lines are negative) and precipitation (shaded); **(b)** zonal wind expansion coefficients; and **(c)** precipitation expansion coefficients. Mode 1 captures the coupled interannual variation in zonal wind over Asia with precipitation over East Asia, with a more northern jet associated with a ‘tripole’ pattern with less rain over central China, and more rain over northern and southern China. We interpret this pattern to be an earlier transition from Meiyu to Summer with a more northward jet. The dashed red lines in (b) and (c) shows the linear least-square trend to the corresponding timeseries.

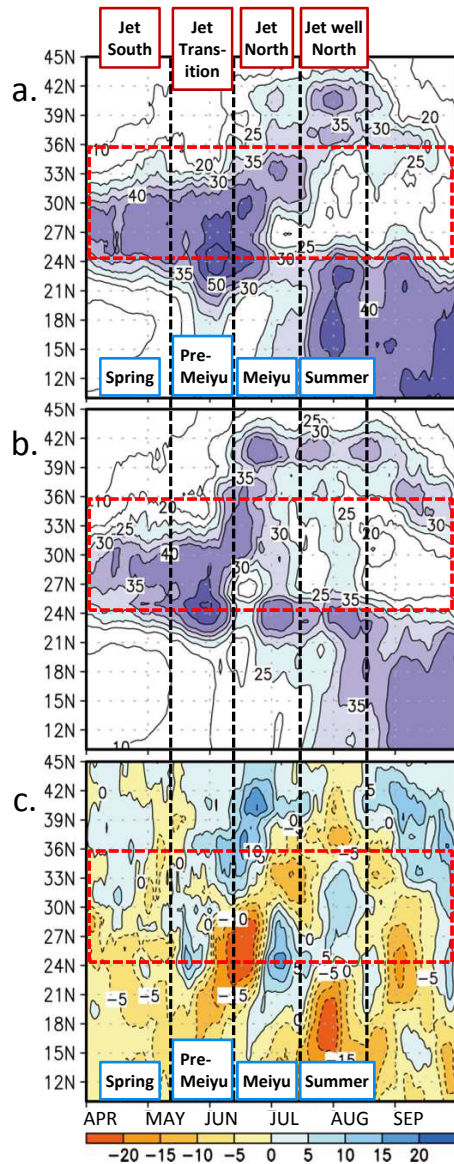


Figure 11. CAM5-simulated latitude-time section of 5-day mean rainfall over eastern China (110°E-120°E, see inset) from April to September. This is to be compared to the observational equivalent in figure 2. **(a)** Preindustrial simulation. **(b)** 11,000ybp simulation. **(c)** Difference (b minus a). They clearly show the earlier onset of the Meiyu, and an extended summer rainfall, in the 11,000ybp simulation compared to the preindustrial. Units of precipitation are mm. For both simulations, the model was integrated for 40 years, and the last 20 years were used to form the climatology.

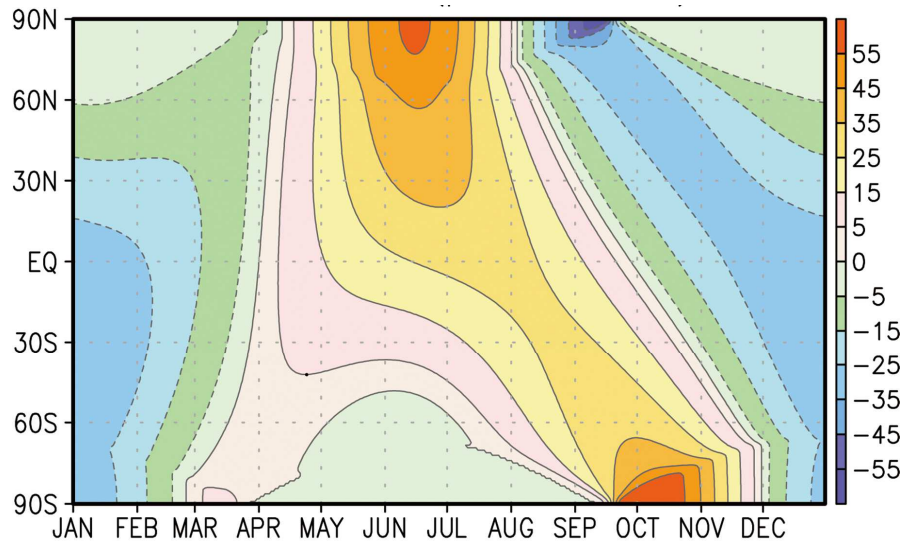


Figure 12. *Top-of-Atmosphere (TOA) changes to insolation between the today (as used by the control simulation) and 11,000ybp. Units are W/m^2 . Between April and September, Northern Hemisphere insolation 11,000 years ago is larger than present, and up to $55W/m^2$ difference at the northern polar regions.*

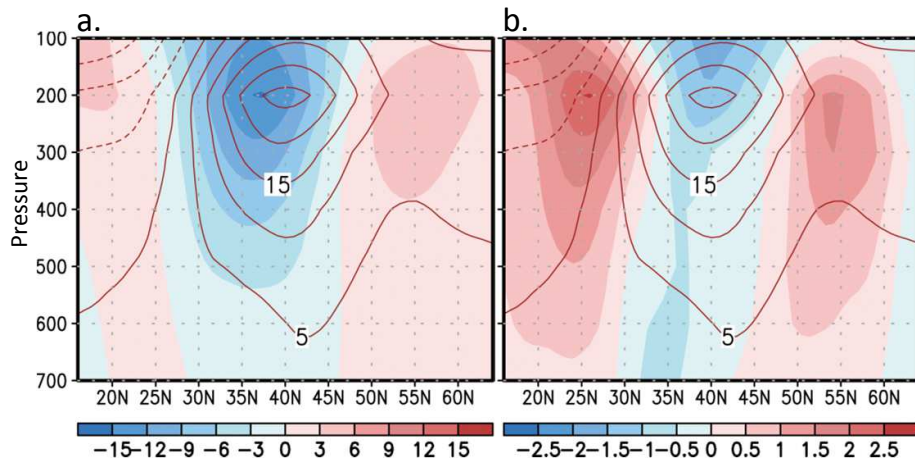


Figure 13. Change in the June-August zonal wind over East Asia as a result of the climate perturbation. Shaded values (units in m/s) are the change to the simulated zonal wind averaged over June-August and 100°E-125°E; contours (interval 5m/s) are the climatological winds. **(a)** 11,000ybp run; results indicate a northward shift in mean jet latitude, primarily manifested as a weakening of the jet at the southern edge. The weakening starts around mid-April, is strongest during July, and terminates around mid-September (not shown). **(b)** North Atlantic cooling run; results indicate a southward shift in the mean jet latitude, manifested by weakening of the winds at the mean jet latitude, and strengthening to the south of it. Note that the color scale for (a) is different from that of (b); the westerly changes are substantially larger for the 11,000ybp simulation than for the North Atlantic cooling run.

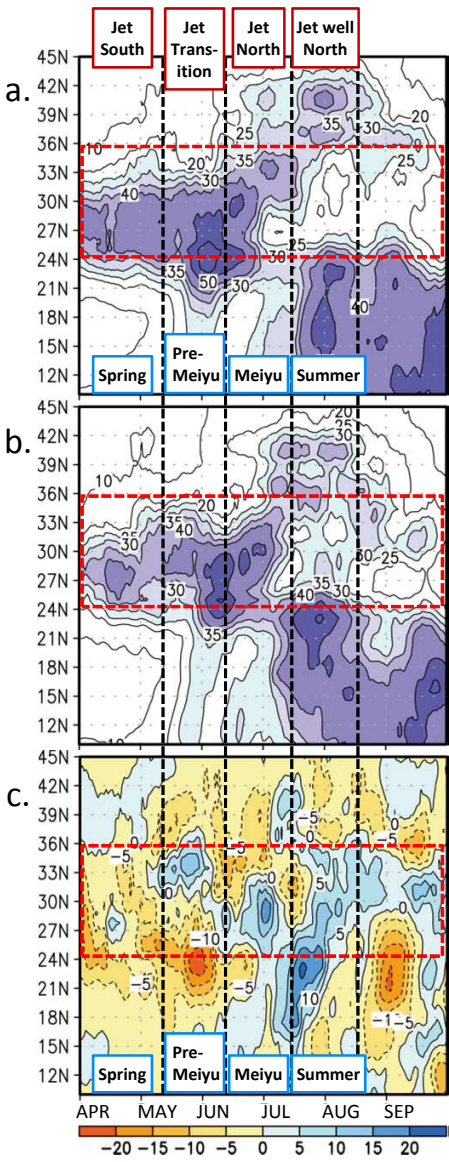


Figure 14. Same as figure 11, but for the North Atlantic cooling run. **(a)** Preindustrial simulation. **(b)** North Atlantic cooling simulation. **(c)** Difference (b minus a). The change is not as clear as for the 11,000ybp run, but do show a delay in the Meiyu onset (as indicated by the ‘dipole’ in precipitation anomalies between the 24°N-33°N latitude band, from June to July; and a delay in the onset of Summer rainfall (north of 33°N). Units of precipitation are in mm.

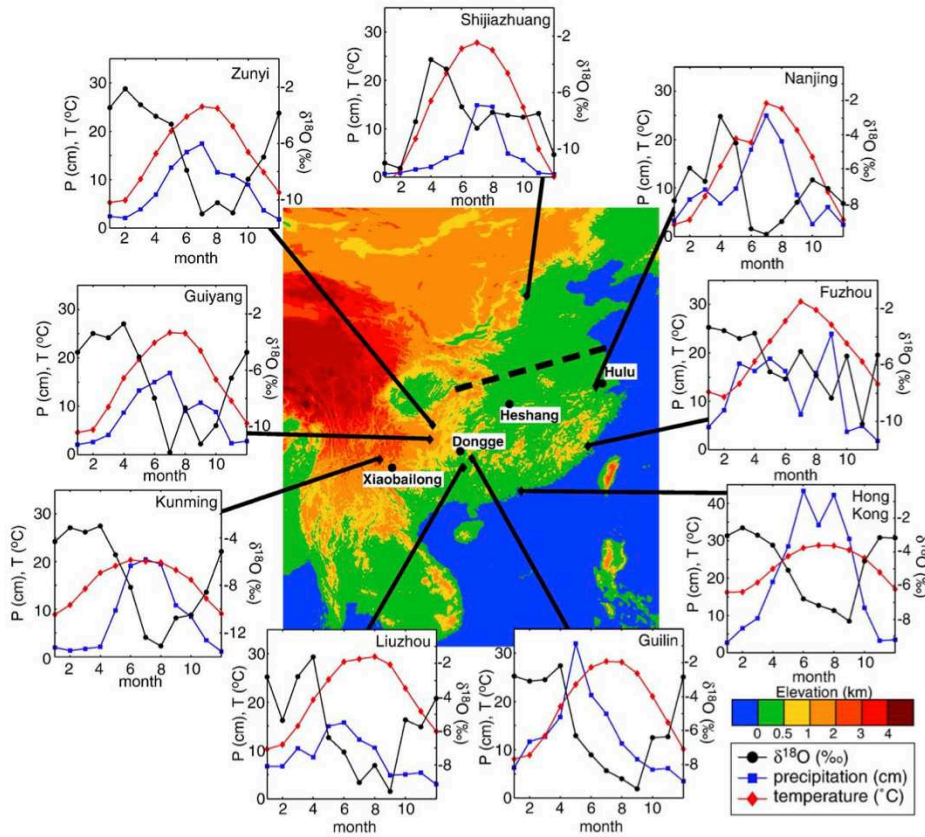


Figure 15. Elevation map of China and surrounding areas with locations of GNIP stations. Dongge, Hulu, Heshang, and Xiaobailong cave locations are marked with black dots. Insets show seasonal cycles of temperature (red lines, units of °C, left axis), precipitation (blue lines, units of cm/month, left axis), and $\delta^{18}O_p$ values (black lines, units of ‰, right axis). Dashed line indicates approximate northern limit of Meiyu front. Figure from Dayem et al. [2010].

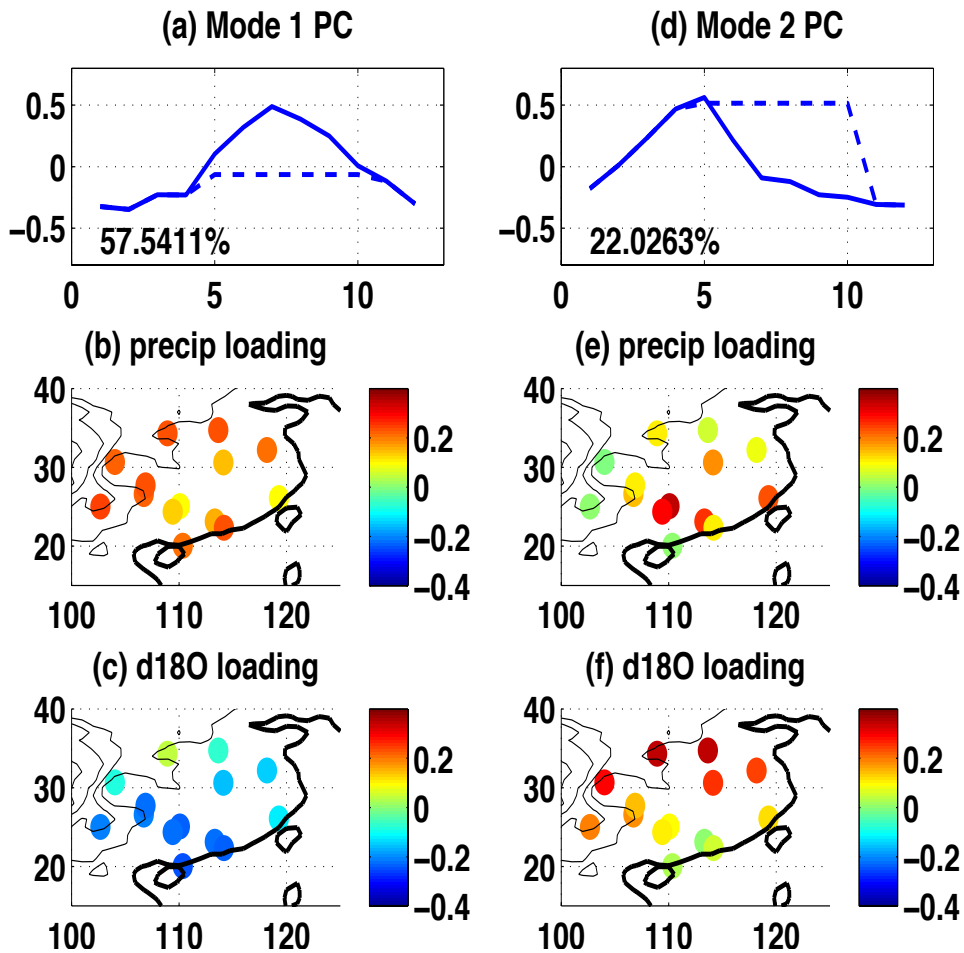
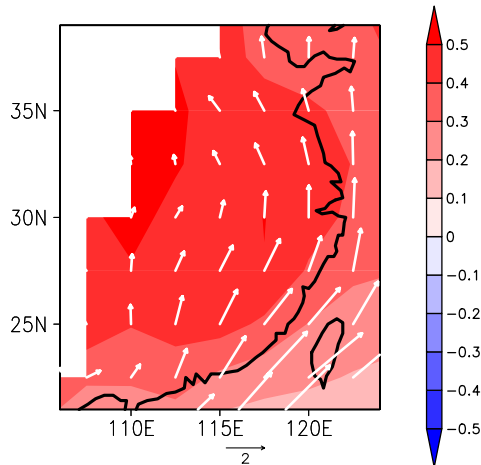


Figure 16. First two modes of a Combined Empirical Orthogonal Function (CEOF) analysis on the monthly mean climatology for precipitation and $\delta^{18}O_p$ for each GNIP station. (a) PC1 (solid line); (b) EOF 1 loading for precipitation; and (c) EOF 1 loading for $\delta^{18}O_p$. (d-f): same as (a-c), but for mode 2. The dashed line shown in (a) and (d) are idealized modifications to the PC to simulate prolonged ‘Spring’ conditions during the summer months (see text for details). The GNIP stations chosen are in the ‘East Asian Monsoon’ domain of 100-130°E and south of 36°S; only stations with elevations < 2km are used. Each of the anomaly (i.e. annual mean removed) precipitation and $\delta^{18}O_p$ fields is normalized locally; then a combined data matrix is formed and the EOF computed. Only modes 1 and 2 are significant, and they are also well separated (according to North’s Rule of Thumb).

Mode 1 (left column) shows a seasonal cycle with high precipitation in the summer for all stations; for $\delta^{18}O_p$, it is lighter in summer, heavier in winter. Mode 2 (right column) maximizes in April-May, and with large positive loadings for precipitation over southeastern China (but positive or near-zero loadings everywhere in general); for $\delta^{18}O_p$, loadings are also all positive but are smallest over southeastern China.

a) Regression on PC1



b) Regression on PC2

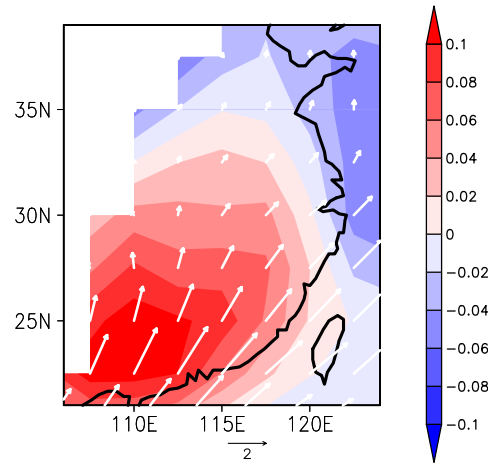


Figure 17. Lower tropospheric moisture transport and specific humidity associated with the EOFs in figure 16. Shown are the regressions of the normalized PC on monthly climatological 925mb u_q and v_q (reference vector is 2(m/s)(g/kg) per unit standard deviation of the PC) and specific humidity (color scale units are g/kg per unit standard deviation of the PC). **(a)** Regression on PC1; and **(b)** on PC2. They show that while EOF1 is associated with low-level moisture transport from the south penetrating well into central China, moisture transport associated with EOF2 is limited to southern China. Moisture transport and specific humidity fields are from NCEP reanalysis, and the climatology is computed over 1979-2012.

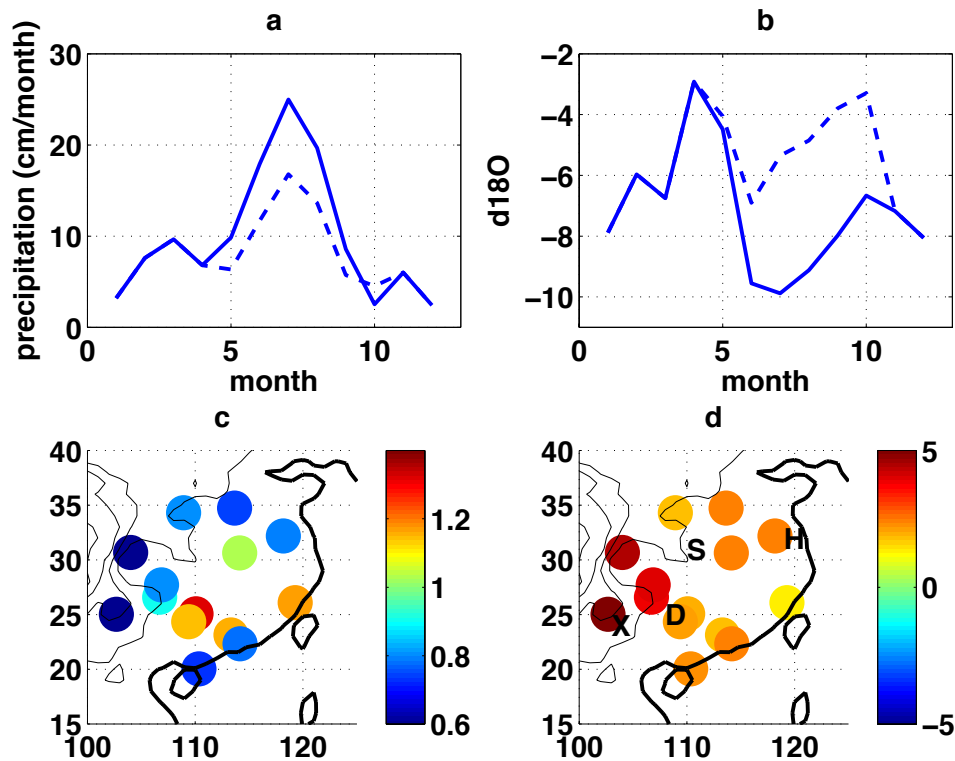


Figure 18. Changes to the station GNIP climatological precipitation and $\delta^{18}O_p$ associated with prolonged ‘Spring’ condition imposed over the summer months of May–October. This was done by changing PCI and 2 loading for May through October to the average for April and May (see dashed lines of figure 16a and figure 16d, respectively); and then reconstructing the station precipitation and $\delta^{18}O_p$. (a) Nanjing climatological precipitation (solid line) and modified (dashed line). (b) Nanjing climatological $\delta^{18}O_p$ (solid) and modified (dashed). (c) Ratio of modified annual rainfall to actual rainfall. (d) Change in the annual mean (precipitation-weighted) $\delta^{18}O_p$, reported as the difference between the modified and actual. The results show that while the actual precipitation amount is variable spatially (they increase over southern China excluding coastal stations but decrease elsewhere), the $\delta^{18}O_p$ is uniformly heavier over all stations, in particular closer to the Meiyu front latitudes. The letters indicate approximate locations of four key cave speleothem sites: Hulu (H), Sanbao (S), Dongge (D), and Xiaobailong (X).

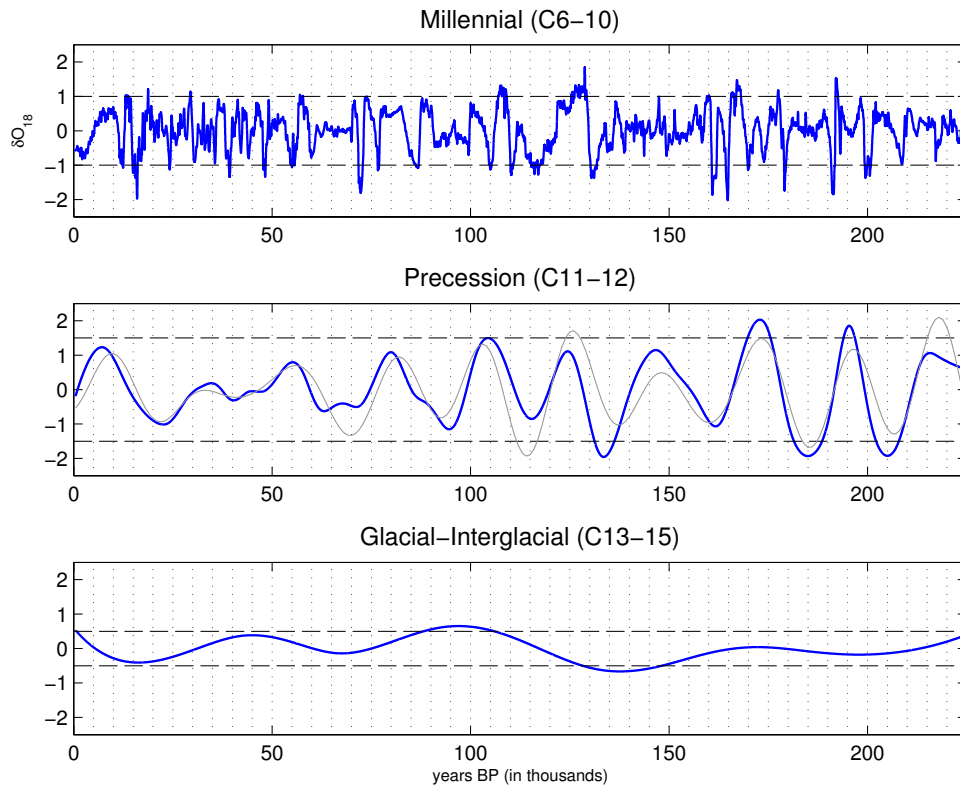


Figure 19. EEMD analysis of the Wang et al. [2008] East Asian speleothem $\delta^{18}\text{O}$ (original data shown in figure 1). The EEMD analysis extracts 15 modes, and modes have been combined to identify with specific timescales of behavior (shown in successive panels). **Top panel:** Millennial timescales (modes 6-10). **Middle panel:** Precessional (modes 11-12); for comparison, the light grey line shows the variation of July 21 insolation at 65°N . **Bottom panel:** glacial-interglacial (modes 13-15). Dashed lines indicate typical peak-to-peak amplitudes of variation for each timescale (± 1 per mil for millennial, ± 1.5 per mil for precessional, and ± 0.5 per mil for glacial-interglacial).

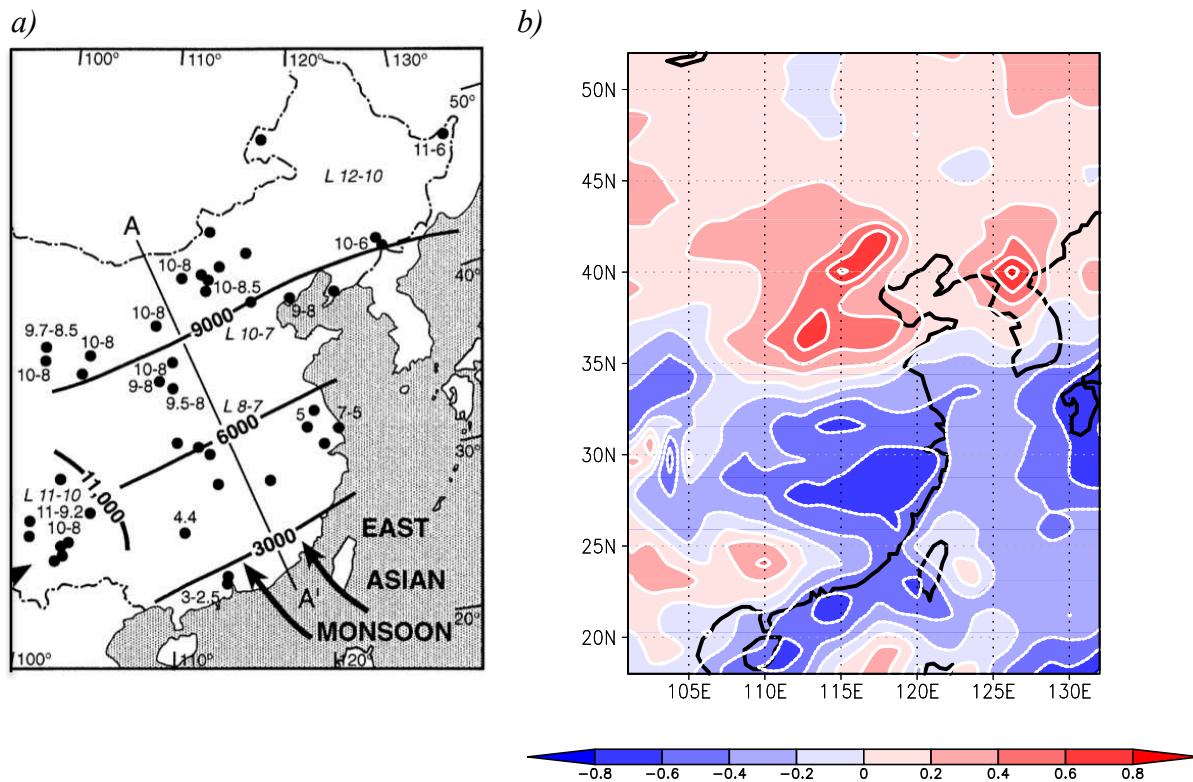


Figure 20. (a) Figure from An et al. [2000], figure 13: their caption reads “Map of China showing position of East Asian Monsoon maximum through time based on paleoclimatic proxy data. Maximum precipitation/effective precipitation occurred ca. 12,000-10,000 yr ago in northeastern China, ca. 10,000-7000 yr ago in north-central and northern east-central China, ca. 8000-5000 yr ago in the middle and lower reaches of the Yangtze River, and ca. 3000 yr ago in southern China. The monsoon maximum dating to ca. 11,000 yr ago in southwestern China is related to the northeastward penetration of the Indian summer monsoon.” (b) Annual mean rainfall difference between the 11,000ybp simulation and present-day control, as described in section 5.1. Units are in mm/day, and contour interval is 0.2mm/d. The simulation shows increased rainfall over northern China and reduced rainfall over central and southern China in this precessional extreme case.

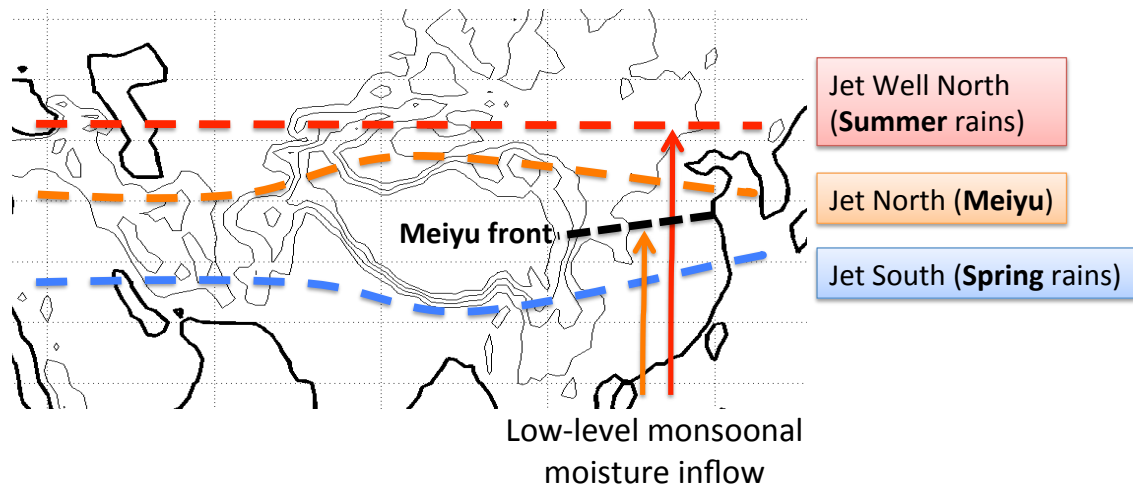


Figure 21. Schematic of the main seasonal stages of East Asian rainfall and relationship to the westerly jet position (colored dashed lines). The thin arrows indicate the extent of northward penetration of low-level monsoonal moisture during the Meiyu (orange arrow) and Summer (red arrow). The black dashed line indicates the approximate position of the Meiyu front. The Jet Transition Hypothesis posits that the timing of these seasonal transitions altered in the past, since the position of the westerlies relative to the Tibetan Plateau changed then.